

CHARACTERIZATION OF LOW-ENERGY ELECTRONIC EXCITED STATES OF
SUBSTITUTED GROUP 8 METALLOCENES

by

JENNIFER SINCLAIR DE MELLO

(Under the Direction of Charles Kutal)

ABSTRACT

Photoinitiated polymerization has found uses in photolithography, coatings, and curing of adhesives. Typical photoinitiators generated cationic or radical species that initiated polymerization. Recently, it has been shown that photochemically generated anions are capable of initiating polymerization. Reinecke's salt (*trans*-Cr(NH₃)₂(NCS)₄⁻) has been shown to undergo ligand substitution releasing a thiocyanate anion. It was shown that this anion could induce polymerization of ethyl 2-cyanocrylate (CA), a common adhesive.

In an effort to look at new classes of anionic photoinitiators, ferrocene (Fc), ruthenocene (Rc), and their benzoyl derivatives were studied. The presence of the electron-withdrawing substituent introduces metal-to-ligand charge transfer (MLCT) character into the excited states of the parent metallocenes. This charge-separated excited state led to relatively efficient metal-ring bond cleavage in the benzoylferrocenes. Interestingly, the benzoylruthenocenes did not undergo metal-ring bond cleavage and instead undergo inefficient photooxidation. The parent metallocenes are also susceptible to photooxidation and follow this pathway more efficiently than the benzoylruthenocenes owing to the ease of oxidizing the metal center.

To complete the story of the group 8 metallocenes, we turned our attention to benzoylosmocene. Electronic absorption and resonance Raman spectral studies revealed that adding the benzoyl group to a cyclopentadienyl ring of osmocene (Oc) caused a significant perturbation of electronic properties. The lowest energy electronic excited states in Oc, which are primarily ligand field in nature, acquired MLCT character in benzoylosmocene (BOc). Both Oc and BOc are relatively photoinert (disappearance quantum yield <10⁻³) in methanol. Irradiating the metallocenes in neat CA initiated the anionic polymerization of the electrophilic monomer. This photoinitiated process resulted from the population of a charge-transfer-to-solvent (CTTS) excited state, which generated the monomer radical anion as the actual initiating species. In an effort to enhance the CTTS mechanism, decamethyl derivatives of ferrocene and ruthenocene were also studied but found to thermally react with CA. Comparison of the present results with those reported previously for the corresponding ferrocene and ruthenocene compounds revealed some interesting similarities and differences in the excited state behavior of the group 8 metallocenes.

INDEX WORDS: photoinitiated anionic polymerization, ferrocene, osmocene, benzoylosmocene, decamethylferrocene, decamethylruthenocene, ruthenocene, cyanoacrylate, benzoylferrocene, benzoylruthenocene, photooxidation, silicon-bridged [1]ferrocenophane, ethane-bridged [2]ferrocenophane

CHARACTERIZATION OF LOW-ENERGY ELECTRONIC EXCITED STATES OF
SUBSTITUTED GROUP 8 METALLOCENES

by

JENNIFER SINCLAIR DE MELLO

B.A., Bellarmine University, 2005

A Dissertation Submitted to the Graduate Faculty of The University of Georgia in Partial
Fulfillment of the Requirements for the Degree

DOCTOR OF PHILOSOPHY

ATHENS, GEORGIA

2010

© 2010

Jennifer Sinclair De Mello

All Rights Reserved

CHARACTERIZATION OF LOW-ENERGY ELECTRONIC EXCITED STATES OF
SUBSTITUTED GROUP 8 METALLOCENES

by

JENNIFER SINCLAIR DE MELLO

Major Professor: Charles Kutal

Committee: Michael K. Johnson
Geoffrey D. Smith

Electronic Version Approved:

Maureen Grasso
Dean of the Graduate School
The University of Georgia
May 2010

DEDICATION

To everyone who has ever told me not to give up, that dreams come true when you fight for them, and that I can dream as big as I want to as long as I have the drive to go for it: this is for you, guys. I love you.

ACKNOWLEDGEMENTS

Many people helped this research project come to fruition. Sowmya Subramanian in Dr. Michael Johnson's group was instrumental for obtaining resonance Raman data. We spent a lot of time, late at night, in the darkness with only the light of the computer monitor, watching the spectra of my compounds. We had a good many conversations and what could have been a bad experience was made less so by the company.

Jeremy Grove from Dr. George Majetich's group helped me greatly with my many synthesis questions and blunders. He taught me in the fashion of Peter Sellers/Dr. Strangelove; to stop worrying about the hazards of certain chemicals and just do the synthesis. Though my syntheses didn't result as expected, I am still grateful to Jeremy for the guidance he was able to provide.

Dr. Matthew Morgan from our group was a good friend throughout the time we spent in lab together. We had a good many conversations about everything life had to offer. He made life in the lab interesting and fun. We kept each other sane when things weren't working and cheered each other on when they were. For that, I am thankful.

My advisor, Dr. Charles Kutal, helped me throughout my time at UGA. He was always quick to give advice. I appreciate the time he spent shaping me into a model chemist.

My family has been my strongest supporters in everything I've done. They have given me hope when things weren't working and celebrated when I'd done well. They told me it would be fine, and, of course, it always was. It is not too much to say my father has been my guiding light. In his mind, there was nothing I couldn't do and because he believed it, so did I. Well, here

it is, Daddy. Proof that your little girl can do whatever she puts her mind to. Thank you for always believing, always pushing, always wanting the best for me.

My husband has been another source of strength. Always supportive and reminding me of the light at the end of the tunnel. My mother, armed with balloons and, if she's really into it, a cowbell, to cheer on every accomplishment with no little amount enthusiasm. Even the smallest hurdle was a great obstacle in her eyes and I am thankful for her support. My sister, though we don't quite understand each other, is always willing to help if needed.

My grandmother symbolizes everything I have accomplished. She came from a one-room schoolhouse in western Kentucky. She was the smartest one in her class and made it all the way to sixth grade. She carried six children and an ailing husband into the world after the war. She was the rock for all of us, and she will be missed. She will always remind me where I came from. Every success I have, I turn to her with pride. This is what we can do, Granma.

I must thank the many friends who keep me sane. Kelly, Stephanie, Sally.... The friends I've made in undergrad in Kentucky who followed me here in spirit. (And those professors and lab coordinators who I still call up time-to-time.) I miss the twang, the Skyline chili, and the daily rides on the elevator we swore would drop us to our doom. I am glad that the girls from high school didn't forget about me though we were separated for many years while we chased after our dreams. We're still running, aren't we? The friends I've made in graduate school who can lend an open ear and share their own grievances. The ones who I'll talk to years from now and we'll agree it wasn't all that bad and high-five each other for sticking it through. The new friends I've made through my husband who remind me that this world has many, many things to offer and all I have to do is grab for them.

Thank you all.

TABLE OF CONTENTS

	Page
ACKNOWLEDGEMENTS	v
LIST OF TABLES	ix
LIST OF FIGURES	x
CHAPTER	
1. INTRODUCTION	1
Photoinitiated Anionic Polymerization	1
Group 8 Parent Metallocenes	4
Benzoyl-Substituted Group 8 Metallocenes	6
Methyl-Substituted Group 8 Metallocenes	8
Group 8 Metallocenophanes	9
Statement of Goals	10
2. MATERIALS AND METHODS	27
General Methods and Materials	27
Synthesis of Benzoylosmocene	28
Synthesis of Ethane-Bridged [2]Ferrocenophane	31
Mass Spectral Analysis	33
Resonance Raman Spectroscopy	33
Nuclear Magnetic Resonance Spectroscopy	34
Relative Rate of Photoinitiated Anionic Polymerization of Ethyl 2-Cyanoacrylate	34

3. CHARACTERIZATION OF THE PHOTOREACTIVITY OF OSMOCENE AND ITS BENZOYL-SUBSTITUTED DERIVATIVE	35
Electronic Absorption Spectra.....	35
Metal-to-Ligand Charge Transfer Character	35
Supporting Evidence of Metal-to-Ligand Charge Transfer Character	36
Evidence of a Donor-Acceptor Complex	37
Photosensitivity of Osmocene and Benzoylosmocene	38
Determination of Quantum Yield Using Nuclear Magnetic Resonance Spectroscopy.....	38
Anionic Photoinitiation of Ethyl 2-Cyanoacrylate	40
Summary	41
4. DISCUSSION ON THE PHOTOCHEMISTRY OF GROUP 8 PARENT METALLOCENES AND THEIR BENZOYL DERIVATIVES	56
Photochemical Mechanism of the Group 8 Parent Metallocenes and Their Derivatives	56
Concluding Remarks.....	58
5. PHOTOOXIDATION OF METHYLATED FERROCENE AND RUTHENOCENE DERIVATIVES.....	65
Electronic Absorption Spectra.....	65
Formation Constants of Donor-Acceptor Complexes	66
6. ETHANE-BRIDGED [2]FERROCENOPHANE.....	78
Attempted Synthesis of Ethane-Bridged [2]Ferrocenophane.....	78
7. CONCLUDING REMARKS.....	80
REFERENCES	83

LIST OF TABLES

	Page
Table 1: Disappearance Quantum Yields of Benzoyl and Parent Group 8 Metallocenes	18
Table 2: Solvent Dependency of the Electronic Absorption Bands of Benzoylosmocene.....	45
Table 3: Resonance Raman Assignments of Osmocene and Benzoylosmocene.....	48
Table 4: ¹ H Nuclear Magnetic Resonance Assignments of Benzoylosmocene.....	51
Table 5: Relative Rates (t_{poly}) of Anionic Photoinitiation of Osmocene and Benzoylosmocene Irradiated with White Light (>290 nm)	54
Table 6: Relative Rates (t_{poly}) of Anionic Photoinitiation of Group 8 Metallocenes.....	55
Table 7: Formation Constants of a Donor-Acceptor Complex Formed Between a Group 8 Metallocene and Carbon Tetrachloride in Acetonitrile:Carbon Tetrachloride Mixtures	77

LIST OF FIGURES

	Page
Figure 1: Structures of Group 8 Metallocenes and Their Derivatives	13
Figure 2: Molecular Orbital Diagram of Ferrocene	15
Figure 3: Metal-to-Ligand-Charge-Transfer Excited State Resonance Structure.....	17
Figure 4: Structures, Tilt, and Deformation Angles of Silicon-Bridged [1]Ferrocenophane and Ethane-Bridged [2]Ferrocenophane.	20
Figure 5: Electronic Absorption Spectra of Silicon-Bridged [1]Ferrocenophane and Ferrocene in Methanol.....	22
Figure 6: Structure of a Bridged [2]Metallocene with Tilt Angle, α , Deformation Angle, δ , and the Angles Along the <i>ipso</i> Carbon and the Bridge, β , Labeled.....	24
Scheme 1: Photochemical Mechanism of Silicon-Bridged [1]Ferrocenophane.	26
Figure 7: Electronic Absorption Spectra of Osmocene and Benzoylosmocene in <i>n</i> -hexane	44
Figure 8: Resonance Raman Spectra of Benzoylosmocene.....	48
Figure 9: Charge-Transfer-To-Solvent Spectra of Osmocene in Solutions of Methanol and Carbon Tetrachloride.....	50
Figure 10: Photoinitiated Anionic Polymerization of a Solution of Osmocene Dissolved in Ethyl 2-Cyanoacrylate.....	53
Figure 11: Possible η^6 -fulvene Resonance Structure in the Excited State of Benzoylruthenocenes and Benzoylosmocene	62
Scheme 2: Photochemical Mechanism of the Group 8 Parent Metallocenes and Their Benzoyl	

Derivatives.....	64
Figure 12: Electronic Absorption Spectra of Decamethylferrocene and Ferrocene in Acetonitrile	70
Figure 13: Electronic Absorption Spectra of Decamethylferrocene Dissolved in Acetonitrile:Carbon Tetrachloride Mixture.....	72
Figure 14: Electronic Absorption Spectra of Decamethylruthenocene and Ruthenocene in Acetonitrile.....	74
Figure 15: Electronic Absorption Spectra of Decamethylruthenocene Dissolved in Acetonitrile:Carbon Tetrachloride Mixture.....	76

CHAPTER 1

INTRODUCTION

Photoinitiated Anionic Polymerization

Photopolymerization, or photoinitiated polymerization, is defined as the initiation of a polymerization process by light. Photopolymerization is used in photocuring of coatings, adhesives, and inks, as well as the creation of masks for electronic components, printing plates, and optical waveguides.¹ Photopolymerization can add a great amount of control in polymer formation. Because light initiates polymerization, it is possible to control both the time and the place of the reaction. The polymerization reaction is only initiated when the light is turned on and only where the light is focused. Since most monomers cannot self-initiate polymerization, photoinitiators and photocrosslinking agents are needed.¹ Photoinitiators absorb the incident radiation and form reactive species that initiate polymerization to give either linear polymers or multidimensional crosslinked networks. There are three types of photoinitiated polymerization mechanisms: free radical, cationic, and anionic photoinitiated polymerization.

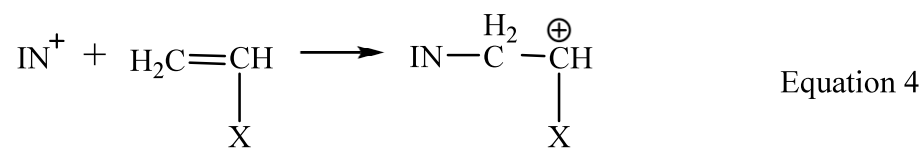
Photoinitiated polymerization begins with a photosensitive compound (PI) that is raised to an electronically excited state (PI^*) by incident radiation (Equation 1). As with most excited state species, PI^* has a very short lifetime on the order of 10^{-6} seconds or less.¹ From this excited state, the molecule can relax back down to the ground state, emitting light and heat, or give a reactive species (IN; Equation 2). This species can then react with the monomer present or other species present in the reaction mixture.



The most commonly photogenerated initiating species are free radicals (IN^\bullet). One reason for this popularity is the sheer number of sources of free radicals that can be generated photochemically and can induce polymerization. However, free radicals have their own problems. One of the drawbacks of free radical initiation is competition of other reactions with the desired polymerization. Unwanted products or deactivation processes occur when the radical initiator reacts with a second radical or impurity instead of the monomer (Equation 3). Since oxygen is a prevalent radical scavenger, owing to its ability to form peroxy radicals ($\text{IN}-\text{O}_2$), this method of photopolymerization must occur under vacuum or inert atmosphere.

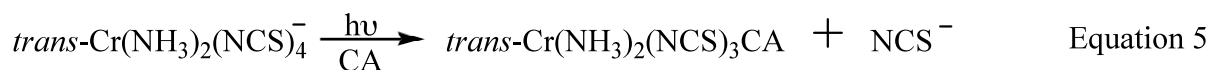


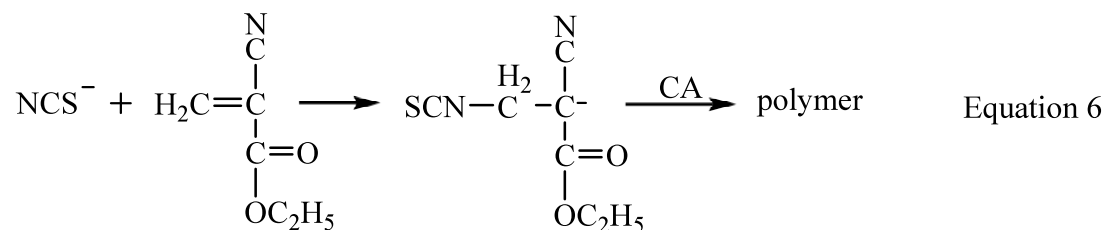
Cationic photopolymerization happens when a photolytically-generated electrophile reacts with monomer to initiate polymerization (Equation 4). Titanium and vanadium tetrachlorides, and silver and gold salts have been used as cationic photoinitiators of epoxy and vinyl ether monomers.^{1,2}



Comparatively, very little work has been done with cationic photopolymers simply because there are few molecules that form a reactive electrophile that upon photolysis can initiate polymerization. Mostly, work has been done with onium salts.^{1,2}

Photoinitiated anionic polymerization had its advent when it was found that Reinecke's salt could induce the polymerization of ethyl 2-cyanoacrylate (CA). This exploratory experiment paired the possibility of a photogenerated anion to induce polymerization with a well-known photochemical system that undergoes the release of an anion. Upon irradiation, Reinecke's salt (*trans*-Cr(NH₃)₂(NCS)₄⁻) undergoes a ligand substitution where a solvent molecule replaces one of the thiocyanate ligands to give a free thiocyanate anion (Equation 5). This anion was able to initiate polymerization of CA by attacking the electrophilic carbon-carbon double bond of the monomer. This thermal reaction yields a carbanion that is stabilized by the neighboring electron-withdrawing groups. The carbanion goes on to attack another monomer unit and initiates polymerization (Equation 6).





The discovery of a transition metal complex that could photochemically generate a reactive anion capable of initiating polymerization opened the door to investigating other similar compounds. It was found that the square-planar platinum(II) acetylacetonate complex released an anion upon irradiation.³ This acetylacetonate anion proceeded to initiate polymerization of CA.

Recently, a detailed study of ferrocene, ruthenocene, and their benzoyl derivatives was undertaken in order to understand their fundamental photochemical and spectroscopic properties as well as gauge their use as practical anionic photoinitiators.⁴ This study was not extended to the heaviest member of the group 8 metallocenes, osmocene, and its benzoyl-substituted derivative. Furthermore, other derivatives of ferrocene and ruthenocene, such as the electron-donating methyl groups or the ring-tilted bridged metallocenophanes, were not considered.

Group 8 Parent Metallocenes

The full compliment of compounds that are of particular interest to this study are shown in Figure 1. To begin, the photochemical and spectroscopic properties of the parent metallocenes, ferrocene (Fc) and ruthenocene (Rc), will be reviewed. Earlier studies of the benzoyl-substituted ferrocenes and ruthenocenes will be treated next. Lastly, the previous knowledge of methyl derivatives and bridged ferrocenophanes will be considered.

Fc adopts D_{5d} symmetry owing to the staggered conformation of the cyclopentadienyl (Cp) rings, though the barrier between the staggered and eclipsed orientations is small. Based on

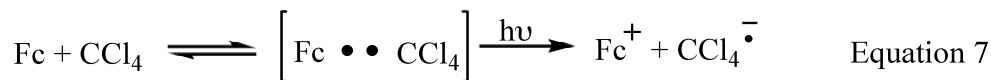
D_{5d} symmetry, assignments of the molecular orbitals can be made (Figure 2). Overlap between the ligand $1e_{1g}$ and metal $3d_{xz}$, $3d_{yz}$ orbitals results in e_{1g} orbitals with ligand character. These orbitals are strongly bonding, in contrast to the $2e_{1g}^*$ which are predominantly metal-based and antibonding in nature.⁵ The $1e_{2g}$ molecular orbitals are mostly metal in character owing to the weak overlap of e_{2g} and $3d_{x^2-y^2}$, $3d_{xy}$ orbitals of the Cp ligand and the iron center, respectively. The highest occupied molecular orbital, $2a_{1g}$, is predominantly metal in nature due to near-zero overlap of the a_{1g} and $3d_{z^2}$ orbitals.

Since they are metal-based, the low-energy excited states discussed above can be treated by ligand field theory. As such, the transitions in the electronic absorption spectra of Fc can be assigned. The ground state is $^1A_{1g}$. Excitation of an electron from a $2a_{1g}$ orbital to the $2e_{1g}^*$ orbital gives rise to an E_{1g} excited state. Two more transitions occur from the promotion of an electron from the $1e_{2g}$ orbital to the $2e_{1g}^*$, giving E_{1g} and E_{2g} excited states. Hence, there are three low-energy ligand field transitions available: $^1A_{1g} \rightarrow a^1E_{1g}$, $^1A_{1g} \rightarrow ^1E_{2g}$, and $^1A_{1g} \rightarrow b^1E_{1g}$.^{5,6} The $^1A_{1g} \rightarrow a^1E_{1g}$ and $^1A_{1g} \rightarrow ^1E_{2g}$ excited states cannot be resolved and give rise to the absorbance band at 442 nm in methanol (MeOH). The other electronic transition, $^1A_{1g} \rightarrow b^1E_{1g}$, appears as an absorbance band at 325 nm in MeOH.⁶ These bands have weak intensity because they are forbidden by the Laporte selection rules. The absorbance bands are also solvent insensitive as the transitions occur on the metal orbitals. Since the ligand orbitals surround the metal orbitals, the metal orbitals have little interaction with the solvent, and, therefore, are solvent insensitive.

Similarly, the excited states for Rc can be considered. The molecule has D_{5h} symmetry with eclipsed Cp rings (Figure 1). Three low-energy, ligand field transitions are expected to occur: $^1A_1' \rightarrow a^1E_1''$, $^1A_1' \rightarrow b^1E_1''$, and $^1A_1' \rightarrow ^1E_2''$.⁷ Similar to Fc, the first two transitions cannot be resolved and give rise to the absorbance at 321 nm in MeOH. The third transition can

be seen as a weak band at 278 nm in MeOH. In the electronic absorption spectra, these transitions are seen to be low intensity and solvent insensitive.

Both Fc and Rc are photoinert in non-halogenated solvents. In contrast, these metallocenes are photosensitive in good electron-accepting solvents such as carbon tetrachloride, CCl_4 ,⁸⁻¹⁰ and tetracyanoethylene.^{11,12} In these solutions, a new absorption feature appears in the electronic absorption spectra. This new absorption is attributed to the formation of a ground-state donor-acceptor complex between the metallocene (donor) and the solvent (acceptor). When it is populated, the excited state of the donor-acceptor complex can lead to a charge-transfer-to-solvent (CTTS) photooxidation. The products of the CTTS photooxidation of Fc and CCl_4 are a ferrocenium cation and a radical anion of the solvent (Equation 7).¹³



This mechanism was of interest because CA is a good electron-accepting solvent. It was thought that the parent metallocenes could generate a reactive anionic species via the photooxidation of the metallocenes and reduction of CA.

Benzoyl-Substituted Metallocenes

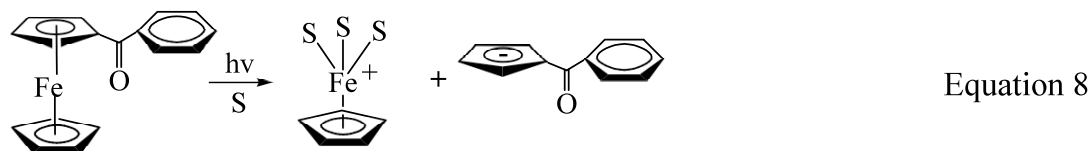
The presence of a benzoyl substituent on one or both of the rings of Fc and Rc leads to marked changes in the spectral properties of the parent metallocenes. The low intensity, solvent insensitive ligand field transitions of the parent metallocenes become high intensity bands. Additionally, the absorbance bands shift to lower energy in more polar solvents compared to non-polar solvents. The benzoyl group allows for mixing of metal-to-ligand-charge-transfer (MLCT) character into the ligand field transitions of the metallocenes. This mixing relaxes the Laporte selection rules and accounts for the greater intensity of the absorption bands.

Furthermore, MLCT leads to solvent sensitivity on account of a charge-separated excited state represented by the resonance structure in Figure 3. The conjugation between the phenyl and Cp rings allows for delocalization of the partial charges, leading to lower transition energy.⁶

Furthermore, more polar solvents are better able to stabilize the partial charges present and thus the absorption bands are shifted to longer wavelengths than those seen in non-polar solvents.

Another consequence of populating this MLCT excited state is the loss of hapticity between the metal and the ring. The bonding has been reduced from η^5 coordination to η^4 . Furthermore, the electrophilicity of the metal center has increased, making it more susceptible to attack from a nucleophile or nucleophilic solvent. These characteristics should enhance the photoreactivity of the low-energy electronic excited states of the benzoyl-substituted group 8 metallocenes.

The benzoylferrocenes were found to undergo ligand dissociation upon irradiation via heterolytic bond cleavage. Upon excitation, the changes in bonding in the excited state facilitate metal-ring bond breaking to yield a half-sandwich iron(II) compound and a benzoylcyclopentadienide anion (Equation 8).^{6, 14-16}



Disappearance quantum yield (Φ_{dis}) data shows that the photodissociation of benzoylferrocene (BFc) occurs a reasonable amount with a value of 0.083 (Table 1).¹⁵ The 1,1'-dibenzoylferrocene (DFc) undergoes metal-ring bond cleavage more efficiently than the monosubstituted derivative.¹⁴

$$\Phi = \frac{\text{moles of product formed}}{\text{moles of photons absorbed}} \quad \text{Equation 9}$$

In a more recent study,¹⁷ it was found that the 1,1'-dibenzoylruthenocene and benzoylruthenocene (DRc and BRc, respectively) had appreciable MLCT in their electronic excited states compared to the ligand field transitions of Rc. However, these compounds do not undergo efficient photodissociation of a benzoylcyclopentadienide anion as indicated by their low quantum yields (Table 1). Knowing that the parent metallocenes are capable of CTTS photooxidation in CCl₄, each of the BRc and DRc compounds was dissolved in various solutions of CCl₄. However, no new absorption feature appears in the electronic absorption spectra. Instead, the shifts that occur in the spectra are attributed to the difference in solvent polarity. A CTTS transition characteristic of a ground-state donor-acceptor complex is suspected to appear at higher energies and is masked by more intense charge-transfer (CT) bands.¹⁷ Therefore, it is possible that the benzoylruthenocenes can undergo CTTS photooxidation.

Methyl-Substituted Group 8 Metallocenes

Decamethylferrocene (DMFc) and its one-electron oxidation product have found uses as a redox couple to calibrate electrochemical studies.¹⁸ The parent compound has also been attached to fullerene in a quest for a charge-transfer complex with novel properties such as superconductivity and ferromagnetism.¹⁹ Interestingly, decamethylruthenocene (DMRc) has been used to form a triple decker, 30 electron sandwich compound.²⁰

Our interest in the methylated metallocenes grew from the knowledge of the photooxidation of the parent metallocenes (Equation 7) and benzoylruthenocenes. In order to enhance the efficiency of photooxidation, electron density is added to the compound via electron-donating methyl groups. Thus, the latter part of this thesis will deal with the formation

of a ground-state donor-acceptor complex between the decamethylmetallocenes and CA, as well as the possibility of CTTS photooxidation leading to anionic polymerization.

Group 8 Metallocenophanes

Silicon- and ethane-bridged ferrocenophanes have shown similar changes in their electronic spectra as those seen for the benzoylferrocenes when compared to ferrocene (Figure 4). Like the benzoyl-substituted ferrocenes, the low-energy excited states of silicon-bridged [1]ferrocenophane (FcSiMe_2) have increased intensity and are red-shifted (Figure 5).²¹ These spectral changes are attributed to the distortion of the complex caused by the bridging ligand. The tilting of the Cp rings reduces the symmetry of the complex from D_{5d} to C_{2v} .²² This loss of symmetry brings the HOMO and the LUMO closer in energy, reducing the energy of the transition.²³ The enhanced intensity of the absorbance bands are due to the relaxation of the Laporte selection rules because of the lower symmetry of the molecule. Unlike the benzoylferrocenes and benzoylruthenocenes, the absorbance bands of FcSiMe_2 are not solvent sensitive. Therefore, there is no evidence of MLCT character in the excited state. However, the metal-ring bond is weakened owing to the ring strain of the compound. Ring strain as measured by both the tilt angle, α , and the distortion angle, δ , leads to a higher possibility of substitution of the Cp ligand (Figure 6).²⁴ Even so, metal-ring bond cleavage is rarely seen in the thermal reaction of FcSiMe_2 .²¹

When solutions of the silicon-bridged ferrocenophane are irradiated in methanol, metal-ring bond cleavage occurs. The photoproduct is obtained by breaking the bond between the metal and ring to give a solvated iron(II) species and the free ligand. Irradiation of FcSiMe_2 also increases the thermal reaction whose product is obtained by breaking the bond between *ipso* carbon and bridging silicon to give a ferrocene-like product (Scheme 1).²¹

The photochemistry of ethane-bridged [2]ferrocenophane ($\text{Fc}(\text{CH}_2)_2$) has not been studied. $\text{Fc}(\text{CH}_2)_2$ has a slightly higher tilt angle (Figure 4)²⁵ owing to the smaller size of carbon compared to silicon. Like the silicon derivative, the thermal reaction of the $\text{Fc}(\text{CH}_2)_2$ involves breaking the bond between the *ipso* carbon on the Cp ring and the carbon of the CH_2 bridge.²⁴ Metal-ring bond cleavage has not been seen thermally. From the outset it may appear that $\text{Fc}(\text{CH}_2)_2$ and FcSiMe_2 should have similar photochemistry however, the electron-donating properties of the ethane bridge cannot be dismissed. Due to the electron-donating properties of the ethane bridge, the bond between the Cp ring and the bridging carbon is stronger in the ground state.²⁴ Breaking of the *ipso* carbon might be less efficient due to stronger residual bonding between the Cp ring and carbon in the excited state. In this way, the thermal reaction, as seen in the photochemistry of the silicon derivative (Scheme 1), may occur less than the photochemical pathway of metal-ring bond breaking upon irradiation. Thus, the ethane bridge could lead to more metal-ring bond cleavage than was seen in the study of FcSiMe_2 .

Statement of Goals

The Kutal group entered the world of group 8 metallocenes with the idea of looking at systems that could function as practical anionic photoinitiators of polymerization. The benzoylferrocenes were quite promising with the release of a benzoylcyclopentadienide anion upon irradiation. In contrast, the benzoylruthenocenes did not undergo efficient metal-ring bond cleavage. Instead, they followed a CTTS photooxidation pathway available to the parent metallocenes.

With this knowledge base, we undertook the study of the heaviest of the group 8 metallocenes, osmocene (Oc), in order to complete the story and learned more about the fundamental photochemical and spectroscopic properties of this group. We also looked at the

methylated metallocenes to study the effect of the electron-donating groups on the photooxidation pathway. Finally, we also decided to look at the properties of the ethane-bridged [2]ferrocenophane to see what affect the ring strain would have on the photochemistry. Our research goals were:

- Attempt to synthesize the previously unreported dibenzoylosmocene.
- Determine if the presence of a benzoyl group on the Cp rings of Oc introduces MLCT character into the low-energy excited states of the metallocene.
- Probe the bonding in the excited state via resonance Raman spectroscopy.
- Determine the efficiency of heterolytic metal-ring bond cleavage of benzoylosmocene (BOc) by calculating a quantum yield.
- Measure the extent to which Oc forms a ground-state donor-acceptor complex in good electron-accepting solvents.
- Determine the ability of Oc and BOc to photochemically initiate polymerization of CA.
- Measure the extent to which DMFc and DMRc form a ground-state donor-acceptor complex in good electron-accepting solvents.
- Determine the ability of DMFc and DMRc to photochemically initiate polymerization of CA.
- Classify the low-energy electronic transitions of $\text{Fc}(\text{CH}_2)_2$.
- Test for solvent sensitivity of $\text{Fc}(\text{CH}_2)_2$ as evidence of a charge-separated excited state.
- Determine the quantum efficiency of heterolytic metal-ring bond cleavage of $\text{Fc}(\text{CH}_2)_2$ by calculating a quantum yield.
- Determine the ability of $\text{Fc}(\text{CH}_2)_2$ to initiate polymerization of CA photochemically.

Figure 1:
Structures of Group 8 Metallocenes and Their Derivatives

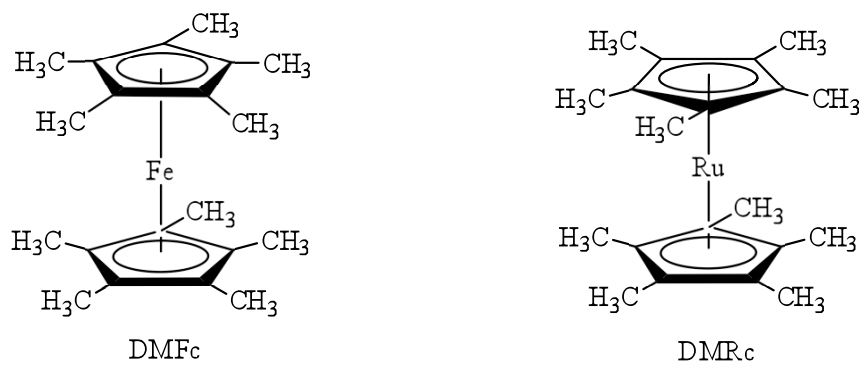
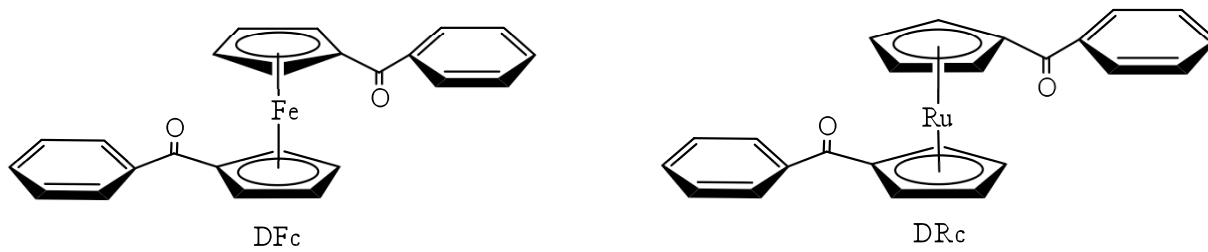
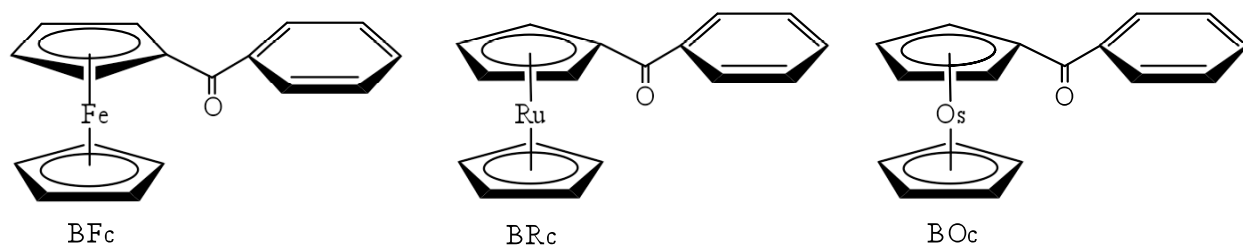
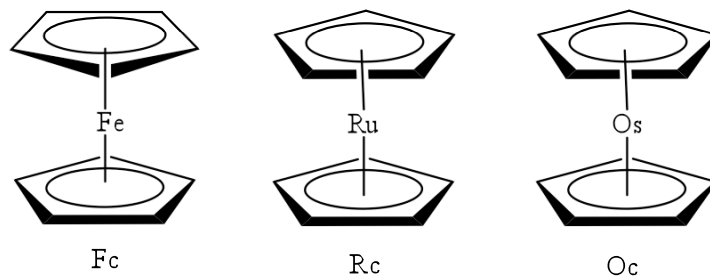


Figure 2.

Molecular Orbital Diagram of Ferrocene. The box highlights the orbitals of the low-energy excited states.⁶

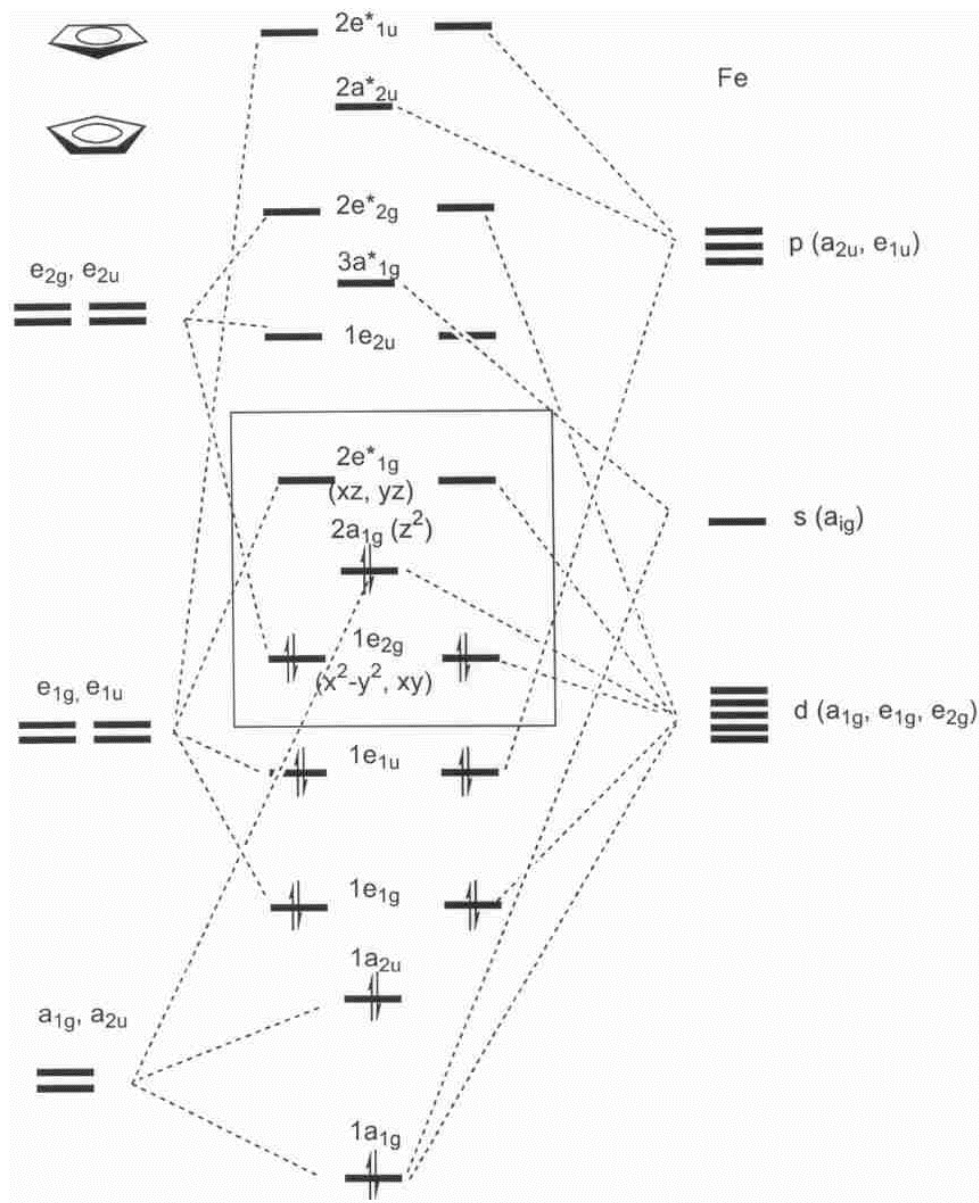
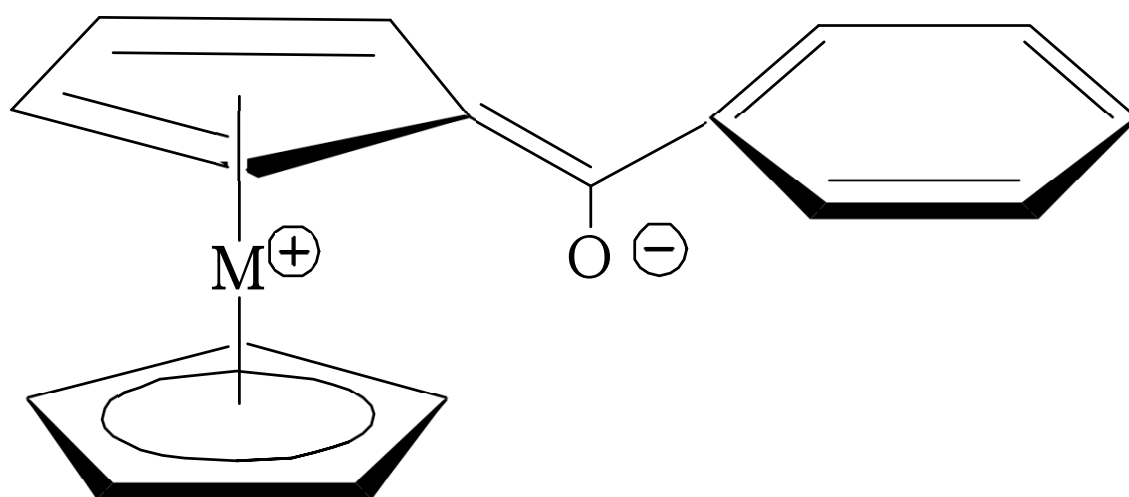


Figure 3.

Metal-to-Ligand-Charge-Transfer Excited State Resonance Structure⁶



$M = Fe, Ru$

Table 1. Disappearance Quantum Yields of Benzoyl and Parent Group 8 Metallocenes

Sample	Φ_{dis}
BFc ¹⁵	0.083 ± 0.01
DFc ¹⁵	0.42 ± 0.06
Fc ⁶	< 1 x 10 ⁻³
Rc ⁶	
BRc ⁶	
DRc ⁶	

Figure 4.

Structures, Tilt, and Deformation Angles of Silicon-Bridged [1]Ferrocenophane and Ethane-Bridged [2]Ferrocenophane. The structural parameters α and δ are defined in Figure 6.

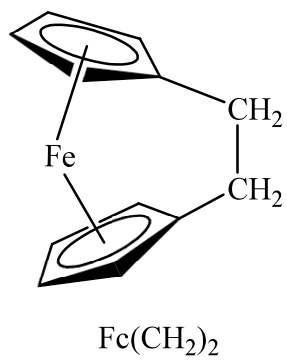
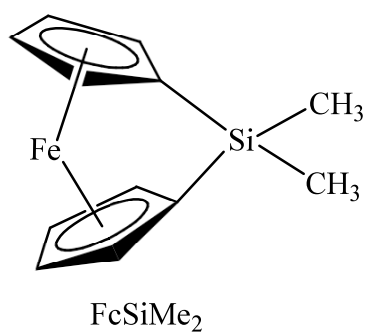


Figure 5.

Electronic Absorption Spectra of Silicon-Bridged [1]Ferrocenophane and Ferrocene in Methanol.

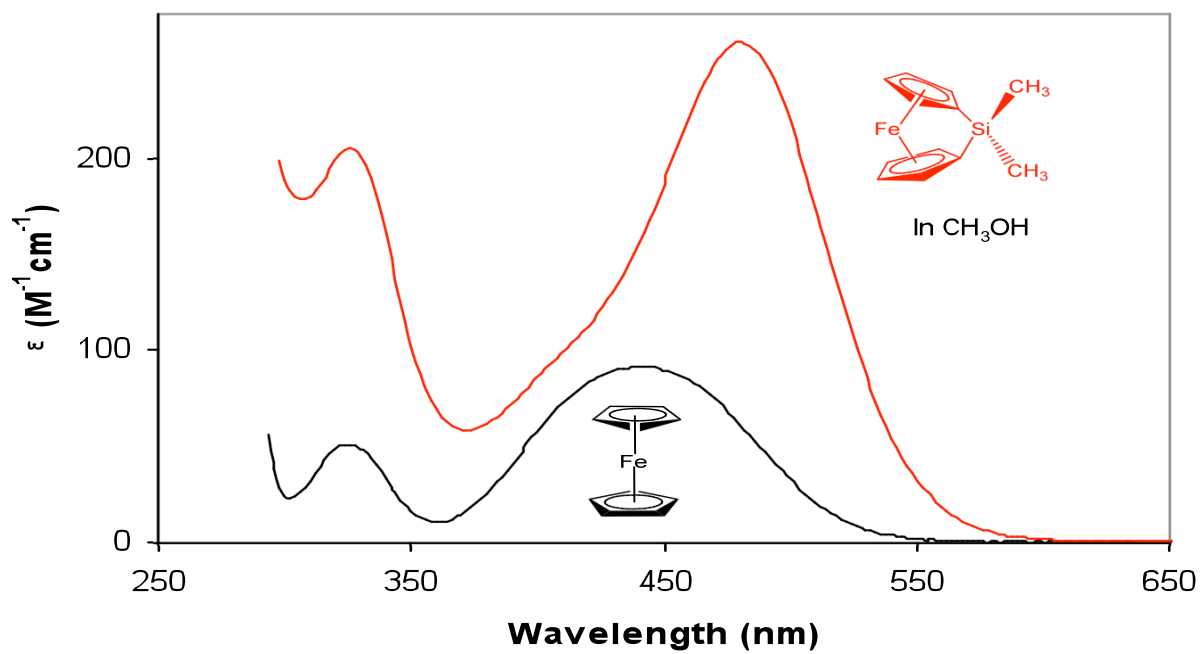
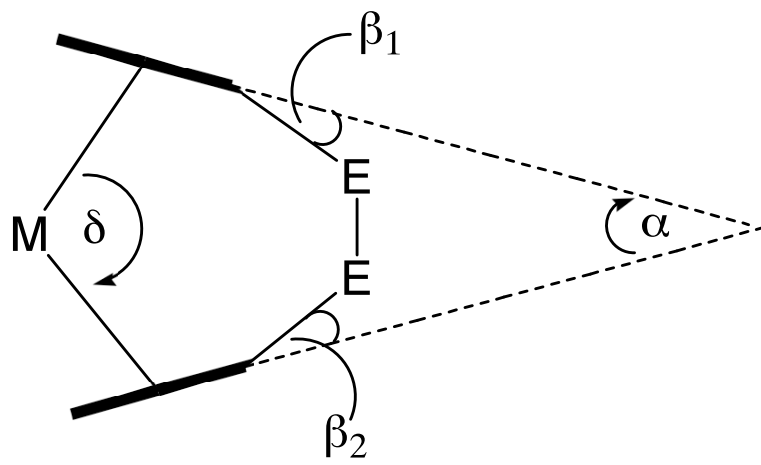


Figure 6.

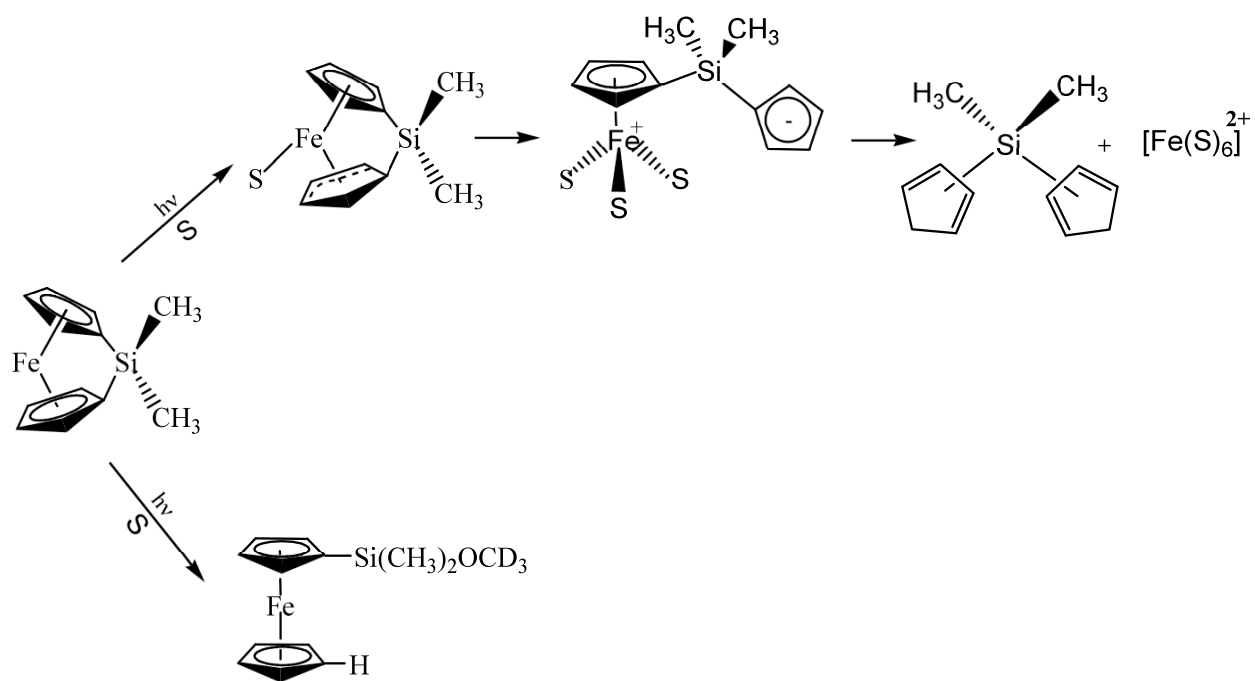
Structure of a Bridged [2]Metallocene with Tilt Angle, α , Deformation Angle, δ , and the Angles

Along the *ipso* Carbon and the Bridge, β , Labeled.²⁶



Scheme 1.

Photochemical Mechanism of Silicon-Bridged [1]Ferrocenophane. The first pathway is that of metal-ring bond cleavage and is only seen upon photoexcitation. The second pathway is the photoaccelerated thermal reaction.



CHAPTER 2

MATERIALS AND METHODS

General Materials and Methods

General Reagents:

Osmocene (Oc; 99.9%, Strem), decamethylferrocene (DMFc; 97%, Aldrich), and decamethylruthenocene (DMRc; 97%, Aldrich) were used as purchased without further purification. *Anal.* Calcd. for C₁₀H₁₀Os (Oc): C, 37.49; H, 3.15. Found: C, 37.69; H, 3.18. *Anal.* Calcd. for C₂₀H₃₀Fe (DMFc): C, 73.62; H, 9.26. Found: C, 73.71; H, 9.34. *Anal.* Calcd. for C₂₀H₃₀Ru (DMRc): C, 64.66; H, 8.13. Found: C, 64.68; H, 8.10.

For the synthesis of BOc, HPLC grade chloroform (99.9%, Fisher) was dried over CaH₂ and distilled under argon. The initial (10%) and final (10%) cuts were discarded, and the distilled solvent was used immediately. For the synthesis of Fc(CH₂)₂, spectral grade *n*-pentane (99.9%, Fisher), tetrahydrofuran (THF; 99.9%, Fisher) and *n*-hexane (95%, Fisher) were dried over CaH₂ and distilled under argon. The initial (10%) and final (10%) cuts were discarded. The distilled solvents were stored over activated molecular sieves. Hexamethylphosphoramide (HMPA; 99%, Aldrich) was purified through freeze-pump-thaw cycles. Dicyclopentadiene (95%, Acros Organics), sodium cubes (99.95%, Aldrich), 1,2-dibromoethane (98%, Aldrich), *n*-butyllithium (2.5M in hexanes, Acros Organics), and anhydrous iron(II) chloride (98%, Aldrich) were used as received. All solvents that were used in electronic spectroscopy and photolysis experiments were of spectroscopic grade and used as received. Anhydrous aluminum chloride (99.99%; Aldrich) and benzoyl chloride (99%, Aldrich) were used as purchased. Aluminum chloride was stored

with desiccant in an argon-filled glovebox. All glassware used for synthesis and making solutions for measuring the rate of polymerization in ethyl 2-cyanoacrylate (CA, 99.9%, Loctite) was dried in a 170 °C oven overnight. Methanol-d₄ (99.8+ % D, 0.03 % v/v tetramethylsilane; Aldrich, Lot# 343803-5G) was used for ¹H NMR experiments.

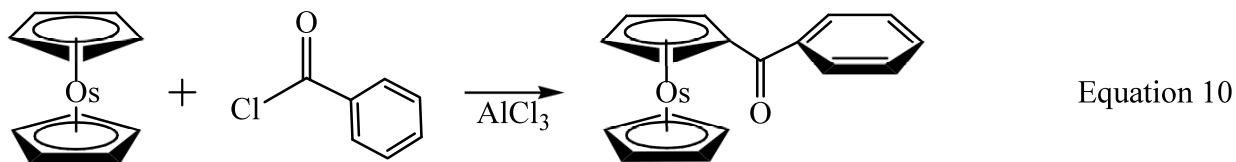
Electronic Spectra:

Electronic absorption spectra were recorded at room temperature (23 ± 3 °C) on a Cary 300 spectrophotometer in 1 cm cells. The cells were made of quartz or optically transparent methacrylate.

Photolysis Equipment:

Continuous photolysis experiments were performed with an Illumination Industries 200-W high-pressure mercury arc lamp. A 365 nm or 313 nm narrow band-pass (10 nm at half-height) interference filter was used to isolate the indicated wavelengths in photochemical studies of BOc and Oc, respectively. The intensities at these wavelengths were measured by ferrioxalate actinometry.²⁷ Polychromatic light of wavelengths >290 nm was obtained by passing the full output of the lamp through Pyrex glass.

Synthesis of Benzoylosmocene



Synthesis of BOc by published procedures²⁸ gave very low yields. Hence, the synthesis was changed slightly based on those previously used to synthesize the benzoylruthenocenes¹⁷ to try to improve yield as well as possibly produce the disubstituted metallocene. Using a larger ratio of Oc:C₆H₅C(O)Cl:AlCl₃, higher boiling solvent, refluxing for a longer period of time,

making use of cannulas, and adding a final separation with ether were major changes made to Rausch's original synthesis. While we were able to improve the yield of monobenzoylosmocene, we saw no signs of the disubstituted osmocene.

In a glovebox, 1.162 mL (10.02 mmol) of benzoyl chloride and 1.336 g (10.02 mmol) of aluminum chloride were added to a 100 mL two-neck, round bottom flask fitted with a reflux condenser and equipped with a stirbar. The apparatus was then removed from the glovebox and placed in a fume hood. To a 50 mL round bottom flask was added 0.500 g (1.56 mmol) of Oc, and the flask was flushed with argon for 15 minutes. A cannula was used to add 20 mL of distilled chloroform to solid Oc. This solution was stirred until the Oc had completely dissolved. The solution was added via cannula to the mixture of aluminum chloride and benzoyl chloride while stirring. This solution was refluxed under argon for 47 hours and then allowed to stir at room temperature for another 7 hours. The solution was poured over 20 g of ice and then the resulting mixture was put into a separatory funnel. The solution formed two layers: a top, yellow water layer and a bottom, dark red organic layer. The fact that BOc prefers the aqueous layer over the organic layer is a testament to the increased basicity of the osmium center. Since BOc was in the top layer, the organic layer was removed. The water layer was washed 3 times with equal portions of chloroform. A final wash with diethyl ether extracted some impurity and the water was collected. A Kimwipe was secured around the mouth of the flask and the solution placed in the back of the fume hood.

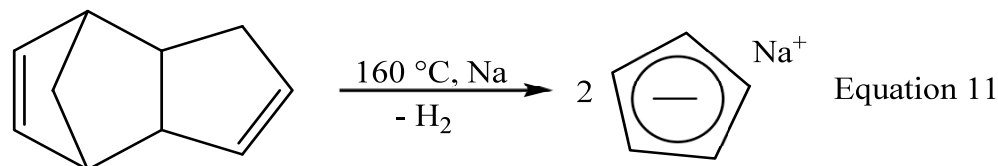
After 3 days, yellow needles separated out of the solution. The water was removed using a rotary evaporator and the wet crystals were placed in a vacuum desiccator to remove the rest of the solvent. The crude product was dissolved in warm benzene and filtered while warm. Thin-layer chromatography (TLC) of the filtrate was performed using alumina sheets and a 50:50

ether/hexane solvent. This procedure afforded only unreacted Oc, BOc, and an impurity. This impurity ran slower than BOc and was credited to an organic molecule, possibly benzoic acid. Petroleum ether was added to the hot, filtered benzene solution and the solution was stored at -15 °C overnight. Clusters of crystals formed and were filtered using a funnel with glass frit. The reaction yielded 0.142 g (21.5% yield) BOc as yellow needles. The mp was 132.0 - 132.8 °C, in good agreement with previously reported values.²⁸ Electrospray ionization mass spectrometry (ESI-MS) of the final product showed evidence of the parent ion $[M+H]^+$ at 427 m/z as well as a sodium adduct $[M+Na]^+$ at 449 m/z. Both of these peaks had an isotope pattern consistent with an osmium containing compound. There was not a peak at 529 m/z, therefore it is doubtful that any of the protonated 1,1'-dibenzoylosmocene molecule $[M+H]^+$ was formed. *Anal.* Calcd. for $C_{17}H_{14}Os$ (BOc): C, 48.01; H, 3.32. Found: C, 48.12; H, 3.41.

One reason the disubstituted benzoyl compound has not been made is because Oc has a higher basicity than Fc and Rc, making the Cp rings less susceptible to electrophilic attack.²⁸ Because most of the electron density sits on the metal versus the rings, the Cp rings are less likely to undergo electrophilic substitution. Furthermore, the benzoyl group is electron-withdrawing and delocalization allows its effects to be felt by the unsubstituted Cp ring.²⁹ The unsubstituted Cp ring is then more stable toward a second electrophilic attack during the Friedel-Crafts acylation. In this way, the monosubstituted osmocene inhibits the synthesis of a disubstituted benzoyl derivative.

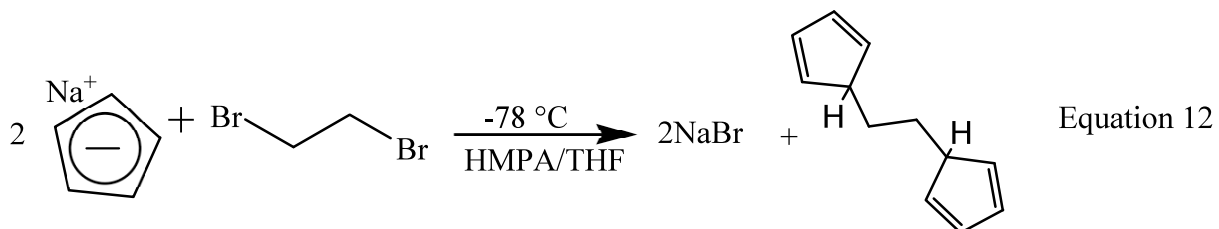
Synthesis of Ethane-Bridged [2]Ferrocenophane

Step 1: Sodium Cyclopentadienide (NaCp)



NaCp ordered as a solution from Sigma Aldrich did not give results. A published synthesis³⁰ illustrates a newer, simpler preparation for the salt. In the fume hood, 3.9 g of sodium metal (0.71 mol) were added to 160 mL of dicyclopentadiene (1.19 mol) and hooked up to a reflux condenser with a bubbler. This solution was heated to 160 °C and refluxed overnight under a steady stream of argon. Vigorous stirring was necessary to ensure the reaction went to completion. In the glovebox, the white solid was filtered and washed with pentane three times, during which it turned brown, and dried under vacuum.

Step 2: 1,2-Dicyclopentadienylethane



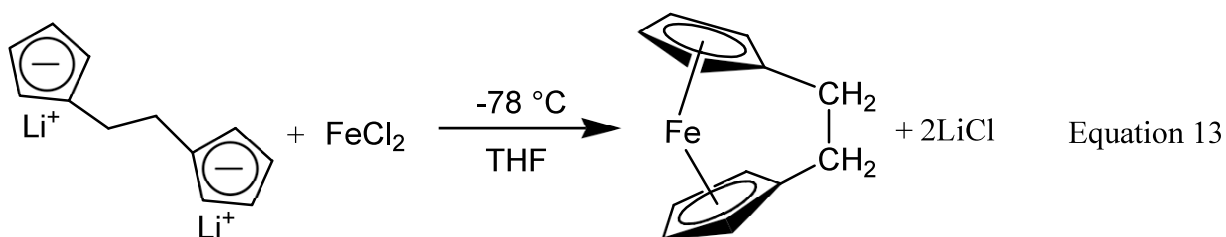
Modifications of a previous synthesis³¹ yielded the lithiated Cp rings that wrap around a iron(II) center to give the bridged ferrocene. First, in the glovebox, 10 g of previously prepared NaCp (0.114 mol) were placed in a round bottom flask. To this flask, 60 mL of THF and 40 mL of HMPA (0.230 mol) were added. Two molar equivalents of HMPA for every mole of NaCp were necessary to increase the reactivity of the Cp anion. Combining NaCp, THF, and HMPA gave a dark red solution. An addition funnel was fitted to the top of the round bottom flask. Into the addition funnel was placed 4 mL of 1,2-dibromoethane (0.046 mol). This solution was cooled to -78 °C and 1,2-dibromoethane was added over the period of an hour. The solution was then

kept at $-78\text{ }^{\circ}\text{C}$ for another hour before being warmed to $0\text{ }^{\circ}\text{C}$ over third hour. Finally, the solution stirs at $0\text{ }^{\circ}\text{C}$ for a fourth hour.

For all of the following purification steps, the solution was kept as cold as possible with a series of ice baths. Some pieces of glassware were stored in the refrigerator to optimize cooling. The reaction mixture was quenched over ice water and extracted with brine and 200 mL pentane. The water layer was washed with pentane (100 mL x 3) and the pentane collected. The collected pentane was then washed with brine until neutral (50 mL x 6) to remove residual HMPA. The pentane solution was dried over MgSO_4 twice. The first drying was filtered with a Buchner funnel. The second was filtered over glass frit and a 2 cm pad of silica. The pentane was removed in vacuum. The dark red-yellow oil was transferred to a Schlenk flask with 60 mL of hexane and a stirbar. This solution is then cooled to $-78\text{ }^{\circ}\text{C}$.

In order to completely lithiate both Cp rings an excess of *n*-butyllithium must be added. As such, 65 mL of 2.5 M *n*-butyllithium (0.163 mol) were added. The solution was allowed to warm to room temperature and to stir overnight with an argon balloon to allow for changes in pressure. In the morning, the solution was filtered via cannula. The white solid was washed with hexane and then dried in vacuum.

Step 3: Ethane-Bridged [2]Ferrocenophane



In the glovebox, 0.35 g of the lithiated ligand (0.002 mol) and 20 mL of THF were dissolved in an addition funnel. Iron(II) chloride (0.26g, 0.002 mol) was added to a round bottom flask and dissolved in an equal amount of THF. The flask and addition funnel were fitted together and brought out of the glovebox. The flask was cooled to -78 °C before the valve of the addition funnel was opened. The flask was kept at this temperature for three hours. The solution was then warmed to room temperature and stirred overnight.

The next day, THF was removed under vacuum. The solid was sublimed at various temperatures, 40-70 °C under vacuum, but no product was collected from the cold finger. At higher temperatures, the solid at the bottom of the flask turned black.

Mass Spectral Analysis

Instrumentation:

ESI-MS was performed on a Perkin-Elmer Sciex API I Plus single-quadrupole mass spectrometer. Analyte solutions were diluted in methanol and water (1:1). The solution was introduced directly into the spectrometer via an injection loop with a flow rate of 0.2 mL/h. The needle and orifice voltages of the ESI source were 4500 and 60 V, respectively. Mass resolution was 1 unit (u) for a scan range of 100-600 u, a step of 0.2 u, and a dwell time of 4.0 ms.

Resonance Raman Spectroscopy

Instrumentation:

Raman spectra were recorded using an Instruments SA Ramanor U1000 spectrometer fitted with a cooled R943-02 photomultiplier tube. Spectra were recorded digitally using photon counting electronics, and improvements in signal-to-noise ratios were achieved by averaging over multiple scans. Absolute band positions were calibrated using the excitation frequency and are accurate to $\pm 1 \text{ cm}^{-1}$. Lines from a Coherent Sabre 100 10-W argon ion laser were used for

excitation. Plasma lines were removed by using a Pellin Broca prism premonochromator. Scattering was collected at the surface of the samples using 90° scattering geometry and a custom designed sample cell,³² which was attached to the cold finger of an Air Products Displex Model CSA-202E closed cycle refrigerator maintained at 23 K. All spectra were collected in the solid state using sample prepared as KBr disks containing 2% (w/w) K₂SO₄ as an internal standard and 8% (w/w) sample. The disks were attached to the surface of the sample holder using Crycon grease.

Nuclear Magnetic Resonance Spectroscopy

Instrumentation:

¹H NMR spectra were recorded on a Varian Inova 500 MHz spectrometer at 25 °C. The ¹H positions were referenced to tetramethylsilane (TMS) at a chemical shift of 0.00 ppm. In the case of BOc, the resonances at 5.118 ppm and 5.301 ppm were used to gauge the extent of reaction whereas 4.685 ppm was used to analyze the loss of Oc.

Relative Rate of Photoinitiated Anionic Polymerization of Ethyl 2-Cyanoacrylate

Cell Method:

Qualitative studies of the rate of photoinitiated polymerization were conducted with solutions of Oc and BOc in neat CA. A 1 cm rectangular, optically transparent methacrylate plastic cuvette equipped with a magnetic stirbar was filled with 2 mL of solution. The top was parafilm, but no other precautions were taken to keep out air or moisture. The solutions were irradiated with white light at 19 ± 1 °C and t_{poly}, the time required for the viscosity of the solution to increase so that the stirbar was unable to spin, was recorded. Values of t_{poly} were also measured at 365 nm so that light intensity could be determined by chemical actinometry.

CHAPTER 3

CHARACTERIZATION OF THE PHOTOREACTIVITY OF OSMOCENE AND ITS BENZOYL-SUBSTITUTED DERIVATIVE

Electronic Absorption Spectra

The electronic absorption spectra of Oc and BOc in room-temperature *n*-hexanes are compared in Figure 7. Similar to Rc, Oc has D_{5h} symmetry with eclipsed Cp rings. Oc has two transitions, $2a_1 \rightarrow 2e_1^*$ and $1e_2 \rightarrow 2e_1^*$.^{7,33} The spin-allowed transitions show up as shoulders at 310 nm (${}^1A_1' \rightarrow a^1E_1''$) and 280 nm (${}^1A_1' \rightarrow b^1E_1''$), both corresponding to ligand field, spin allowed transitions. A third transition at 251 nm corresponds to a ${}^1A_1' \rightarrow {}^1E_2''$ transition and is obscured by the high intensity CT band at 243 nm.³³ These ligand field transitions are low intensity because of their Laporte forbidden d-d character. Due to the metal-localized nature of these transitions, the bands do not change in intensity or position in solvents of various polarities. The peaks at higher energy, 243 nm and 219 nm, are assigned as CT transitions and surprisingly are not solvent sensitive.

Metal-to-Ligand Charge Transfer Character

When a benzoyl group is added to Oc several spectral changes occur. The absorbance bands are shifted to longer wavelengths (368 nm and 310 nm) and are of greater intensity. Furthermore, these peaks are affected by solvent polarity. They shift to lower energies in higher polarity solvent such as acetonitrile (ACN) versus low polarity solvents like *n*-hexane (Table 2). These transitions cannot be attributed to pure ligand field transitions. Instead, we explain these changes as a direct effect of the benzoyl group. The electron-withdrawing nature of the benzoyl

group allows more ligand character to mix into the metal d-d transitions of Oc, making the low-energy transitions more MLCT-like. Since the transitions are no longer composed of predominately metal character, a relaxation of the Laporte selection rule occurs and the transitions are of higher intensity. We propose that the resonance structure in Figure 3, showing the charge separation of the excited state of BFc and BRc, is also true for BOc. More polar solvents stabilize the separation of charge, resulting in a shift to lower energies in solvents like MeOH and ACN compared to non-polar solvents like CCl₄ and *n*-hexanes.

Supporting Evidence of Metal-to-Ligand Charge Transfer Character

Resonance Raman spectra of solid samples of Oc and BOc at 514-nm (non-resonant) and of BOc at 457-nm (resonant) excitations are shown in Figure 8. The extent of resonance enhancement for discrete bands in the spectrum of BOc using 457-nm excitation was assessed by comparing the Raman intensities relative to that of the 985 cm⁻¹ sulfate vibrational mode. Table 3 gives the assignments for the vibrational modes of Oc and BOc. Assignments for the vibrational modes of Oc were previously published.^{17, 34} BOc vibrational modes were based on those previously reported for BRc and BFc.^{17, 35}

Comparison of the resonant and non-resonant Raman spectra indicates MLCT character and is consistent with the charge distribution of the resonance structure of the electronic excited state (Figure 3). The carbonyl vibrational mode at 1633 cm⁻¹ is greatly enhanced in accord with the expected lengthening of the C-O bond in the electronic excited state. The internal modes of the substituted Cp (Cp'; 1167 and 1439 cm⁻¹) and phenyl rings (Ph; 1000, 1167, 1439, 1578, and 1598 cm⁻¹) also exhibit modest resonance enhancements, as would be expected from the change in conjugation between the two rings in the electronic excited state.

These results are similar to those previously reported for BFc and BRc using resonance Raman spectroscopy.^{17, 35} However, BFc was shown to degrade due to photoinduced loss of the benzoylcyclopentadienide anion and the laser had to be continuously moved across the sample to prevent photodegradation. BRc was not found to photodegrade because it does not lose its benzoylcyclopentadienide ring as readily as the benzoylferrocenes. During these studies with Oc and BOc the laser was not moved from its initial position and there was no evidence of photodegradation over the course of the experiments.

Evidence of a Donor-Acceptor Complex

While Rc and Fc have been shown to form ground state donor-acceptor complexes with good electron-accepting solvents,⁸⁻¹² there is very little work with Oc or BOc except with the strong π -acid tetracyanoethylene.^{11, 12} In studies with Fc and Rc in CCl₄, a CTTS band appeared in the near-ultraviolet region of the spectra (307 nm and 285 nm respectively).^{8,9,36} The spectra of Oc in mixtures of CCl₄ and MeOH are shown in Figure 9. The appearance of a shoulder at 275 nm indicates the formation of a ground-state donor-acceptor complex between CCl₄ and Oc that is not present in methanol. We identify this new feature as a CTTS transition.

When BOc was dissolved in mixtures of CCl₄ and MeOH, no new absorption feature appeared. Instead, the differences in the spectra were attributed to the polarity of the solvent (Table 2). As such, we conclude that any CTTS transitions must occur at higher energies and are effectively masked by high intensity CT bands.

Photosensitivity of Osmocene and Benzoylosmocene

Solutions of Oc in methanol were prepared in millimolar concentrations, bubbled with nitrogen gas for 15 minutes, and irradiated with 313 nm light for 2 hours. Only minor changes

occurred in the spectrum of the photolyzed sample which led us to conclude that Oc is photoinert in non-halogenated solvents.

Deaerated methanol solutions of BOc in millimolar concentrations were irradiated with 365 nm light for 2 hours. There was little variation in the electronic absorption spectrum when compared to the thermal sample kept in the dark. Thus, like its parent metallocene, BOc is photoinert in non-halogenated solvents.

Determination of Quantum Yield Using Nuclear Magnetic Resonance Spectroscopy

To determine the amount of reaction occurring upon irradiation, samples of Oc and BOc were prepared and analyzed using ^1H NMR. A 5 mL stock solution of 6 mM concentration was prepared, 3 mL of which was irradiated at 313 nm in a 1 cm cell for 6 hours. The rest of the sample was put in an NMR tube, wrapped in aluminum foil, and used as a thermal control. The thermal sample was analyzed within an hour of preparing the stock solution and after 6 hours. The solvent, methanol- d_4 , was also analyzed at these times.

Osmocene has one proton peak at 4.685 ppm. Monitoring the change in the area of this peak before and after irradiation allows for the calculation of a percent reaction. After 6 hours of irradiation, no peaks indicative of photoproducts appeared in the spectra. Comparing the thermal reaction at the start and after 6 hours, there was no change in the area of the Oc peak. Therefore, as was seen from the electronic studies, Oc is thermally stable.

As with the Oc, a 5 mL stock solution of 5 mM concentration of BOc in methanol- d_4 was prepared. A 3 mL sample was irradiated using a 365 nm filter for 6 hours, and the remainder placed in an NMR tube and covered with foil immediately. The latter was the thermal sample. The solvent was also analyzed.

BOc, unlike Oc, has many proton peaks which can be seen in Table 4. Assignments were based on previously reported spectra²⁹ and the electron-withdrawing effect of the carbonyl group. The two triplets that correspond to the substituted Cp ring (Cp') were used to determine the percent reaction. There was little change in the thermal sample over the course of 6 hours, thus BOc is thermally stable.

The changes in the peak areas between the irradiated and thermal samples of Oc and BOc were very small. Furthermore, no new peaks appeared in the spectrum after irradiation, therefore no products could be identified. The peak area of Oc at 4.685 ppm went from 3.08 to 2.90 after 6 hours of irradiation, a change of 0.18. The peak area for BOc changed by even less 0.05. This difference was obtained by subtracting the 6 hour irradiated sample, 0.74, from that of the initial peak area of the pair of singlets at 5.301 and 5.118 ppm of the thermal sample, 0.79. These values could not be considered significant changes within the intrinsic error of the NMR. Initially, these peak areas were corrected for changes in concentrations due to solvent evaporation that may have occurred over the 6 hour irradiation period. Similarly, the changes in the MeOH peaks at 3.309 ppm and 3.306 ppm for the Oc and BOc samples respectively were lower than the detection limit of the NMR. Even if solvent had been lost, which would then increase the concentration of Oc or BOc, the effect could not have been seen using NMR.

To define the minimum amount of reaction that could be seen, the digital resolution for the experiments was used. The number of real data points taken with both samples was 32764 over a 7996 Hz sampling width. Thus, the most amount of change that could have been seen was 0.24. To determine the amount of reaction that could be detected for Oc, 0.24 was subtracted from the initial peak area, 3.08. This difference yielded a percent reaction of 7.8 % for Oc. Using this same method for BOc, 0.24 was subtracted from 0.79, the initial area for the pair of singlet

Cp' peaks at 5.301 and 5.118 ppm. This difference gave a percent reaction of 30.4 % for BOc. Minimum disappearance quantum yields were calculated from these values and found to give a limit of $< 7 \times 10^{-3}$ and $< 5 \times 10^{-3}$ for Oc and BOc, respectively.

Anionic Photoinitiation of Ethyl 2-Cyanoacrylate

Without irradiation, solutions containing Oc or BOc in neat CA did not change viscosity for at least 24 h when stored in the dark at room temperature. Therefore, the solutions are thermally stable. Furthermore, after 30 minutes of irradiation, the cell filled with neat CA did not change viscosity when compared to the thermal sample. Thus, very little polymerization occurred without the addition of Oc or BOc.

Upon radiation, Oc solutions polymerized into hard, plastic-like solids. The effective rate of polymerization is expressed as t_{poly} , which is the irradiation time required for the sample to become so viscous the stirbar is no longer able to spin. After the induction time, the solution boils so that bubbles solidify in the hard polymer (Figure 10). These solutions took a long initiation time before reacting quickly after about 250 seconds and with an evolution of heat (Table 5). The behavior of the polymerization after the induction time can be explained. Oc takes a prolonged induction period to overcome the acid preservative in CA that prohibits initial polymerization. To prove this was the case an anionic inhibitor, methanesulfonic acid, was added to a solution of Oc in neat CA (Table 5). The anionic inhibitor increases t_{poly} by acting as an anionic scavenger.

Solutions of BOc in neat CA polymerized after 330 seconds (Table 5). There was an evolution of heat that led to bubbles being formed within the polymer. However, as was noted before, the benzoyl compounds do not undergo metal-ring bond cleavage. As such, only a CTTS photooxidation pathway, where upon excitation BOc is oxidized and CA reduced to give a

radical anion, is available. However, electron-withdrawing benzoyl groups make the molecule harder to oxidize.^{29, 37}

A final experiment was performed to compare the t_{poly} of Oc and BOc with that of Rc and Fc (Table 6). Samples of Oc and BOc in CA were made inside of the glovebox using dry glassware. Methacrylate cells were filled with the solutions and then irradiated with 365 nm light. Ferrioxalate actinometry was performed to determine the average light intensity.

Oc solutions polymerized into a hard, plastic-like solid under 365 nm irradiation. Conversely, after 2 hrs BOc had not polymerized well enough to stop the stirbar from spinning. The solution of BOc, however, had only a thin layer of polymerized material on the side of the cuvette being hit by the radiation. The viscosity of the solution had not appeared to change when compared to a thermal sample.

Of the two compounds, Oc is a better photoinitiator of CA than BOc (Table 6) as BOc is more stable towards oxidation owing to the electron-withdrawing property of the benzoyl group. Nevertheless, they are both poor initiators compared to Rc and DBF.

Summary

Results from this study of Oc and BOc can be compared to previous studies of similar group 8 metallocenes and their benzoyl derivatives.⁶ First, the addition of an electron-withdrawing benzoyl group onto the Cp ring of a parent metallocene leads to perturbations in the low-energy electronic excited state by introducing MLCT character into the ligand field transitions. Thus, all the benzoyl-substituted group 8 metallocenes show an increase in intensity of the low-energy electronic transitions. Also, these absorption bands are solvent sensitive, shifting to lower energies in more polar solvents, indicative of a charge-separated excited state (Figure 3). Resonance Raman spectral data supports this view of the excited state with specific

enhancement of the carbonyl stretching frequency at 1633 cm^{-1} . Charge-separation weakens the metal-ring bond and leaves the metal susceptible to nucleophilic attack. However, BOC, like the benzoylruthenocenes, does not undergo metal-ring bond cleavage. Instead, it forms a ground-state donor-acceptor complex in good electron-accepting solvent and follows a pathway of CTTS photooxidation like the parent metallocenes.

Figure 7.

Electronic Absorption Spectra of Osmocene and Benzoylosmocene in *n*-hexane.

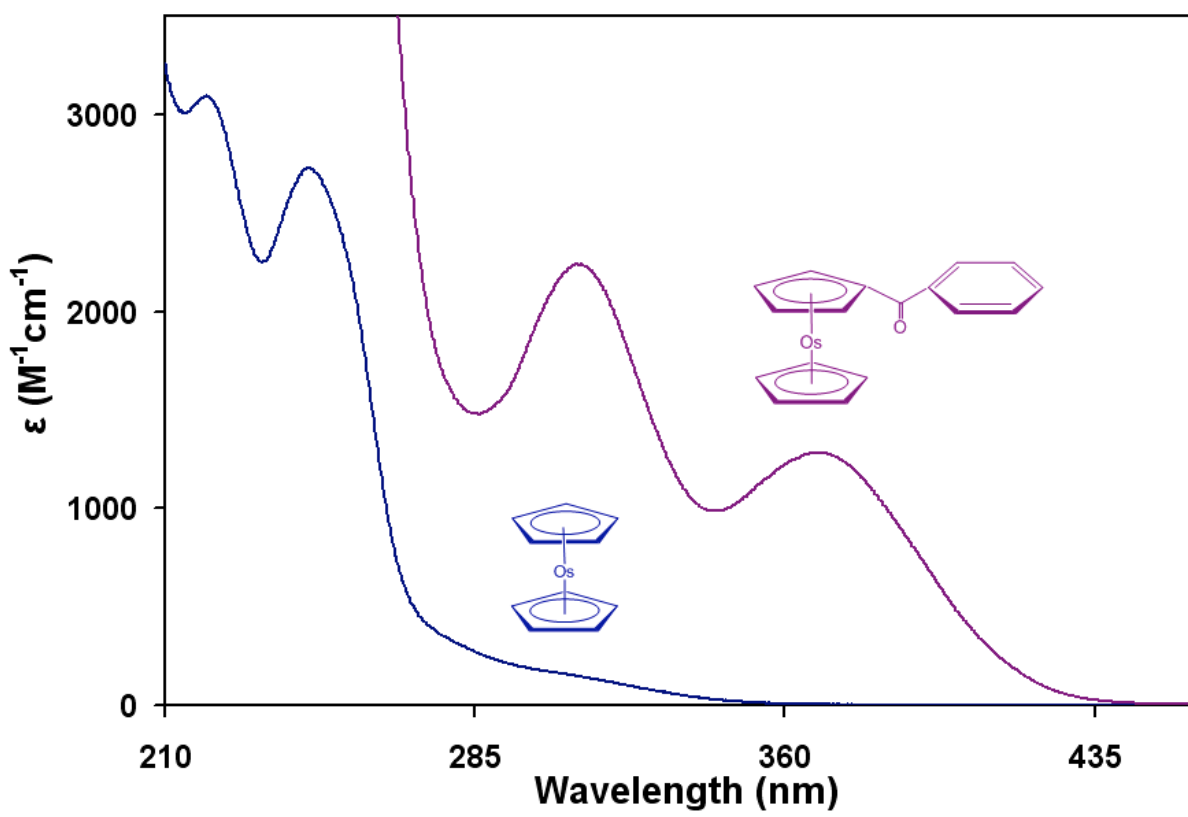


Table 2. Solvent Dependency of the Electronic Absorption Bands of Benzoylosmocene.

Solvent	Dielectric Constant³⁸	λ_{max} , nm (ϵ_{max} , M ⁻¹ cm ⁻¹)	λ_{max} , nm (ϵ_{max} , M ⁻¹ cm ⁻¹)
acetonitrile	37.5	316 (2080)	375 (1290)
methanol	32.7	320 (2190)	379 (1480)
tetrahydrofuran	7.6	314 (2400)	375 (1450)
chloroform	4.81	318 (2260)	380 (1420)
benzene	2.28	315 (2230)	376 (1350)
carbon tetrachloride	2.24	312 (2400)	375 (1270)
<i>n</i> -hexane	1.89	310 (2240)	368 (1280)

Figure 8.

Resonance Raman Spectra of Benzoylosmocene.

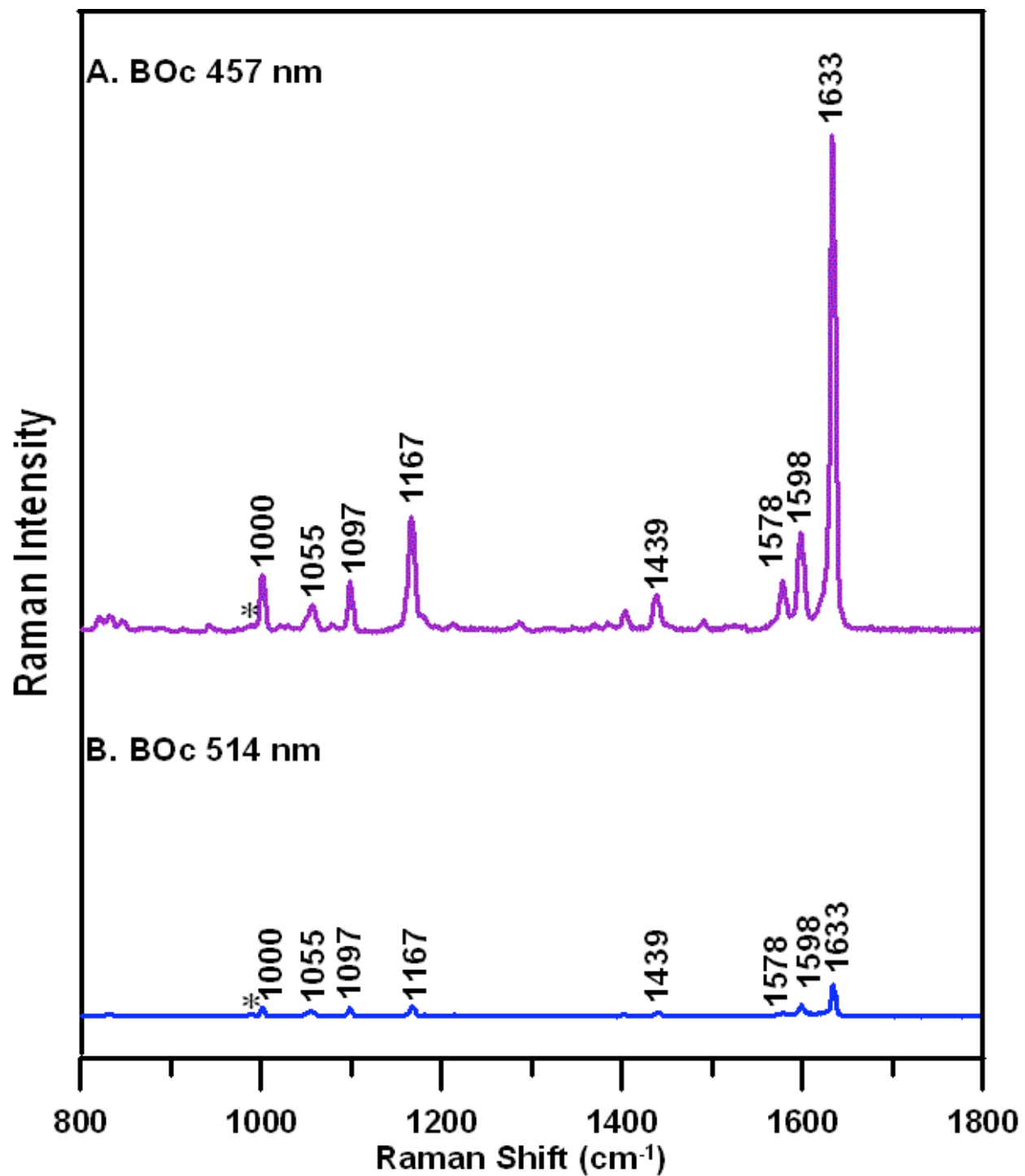


Table 3. Resonance Raman Assignments of Osmocene and Benzoylosmocene.

Oc	BOc	Assignment
1064	1055	$\delta(\text{CCH})_{\text{Ph}}$ or $\delta(\text{CCH})_{\text{Cp}'}$
1094	1097	$\nu(\text{CC})_{\text{Cp}}$
	1167	$\delta(\text{CCH})_{\text{Ph}}$ or $\delta(\text{CCH})_{\text{Cp}'}$
1399	1402	$\nu(\text{CC})_{\text{Cp}}$
	1439	$\nu(\text{CC})_{\text{Cp}'}$
	1578	$\nu(\text{CC})_{\text{Ph}}$
	1598	$\nu(\text{CC})_{\text{Ph}}$
	1633	$\nu(\text{CO})$

Cp' denotes the benzoyl-substituted Cp ring

Ph denotes the phenyl group

Figure 9.

Charge-Transfer-To-Solvent Spectra of Osmocene in Solutions of Methanol and Carbon Tetrachloride. The inset is the difference spectrum showing a new absorption feature indicative of a CTTS transition.

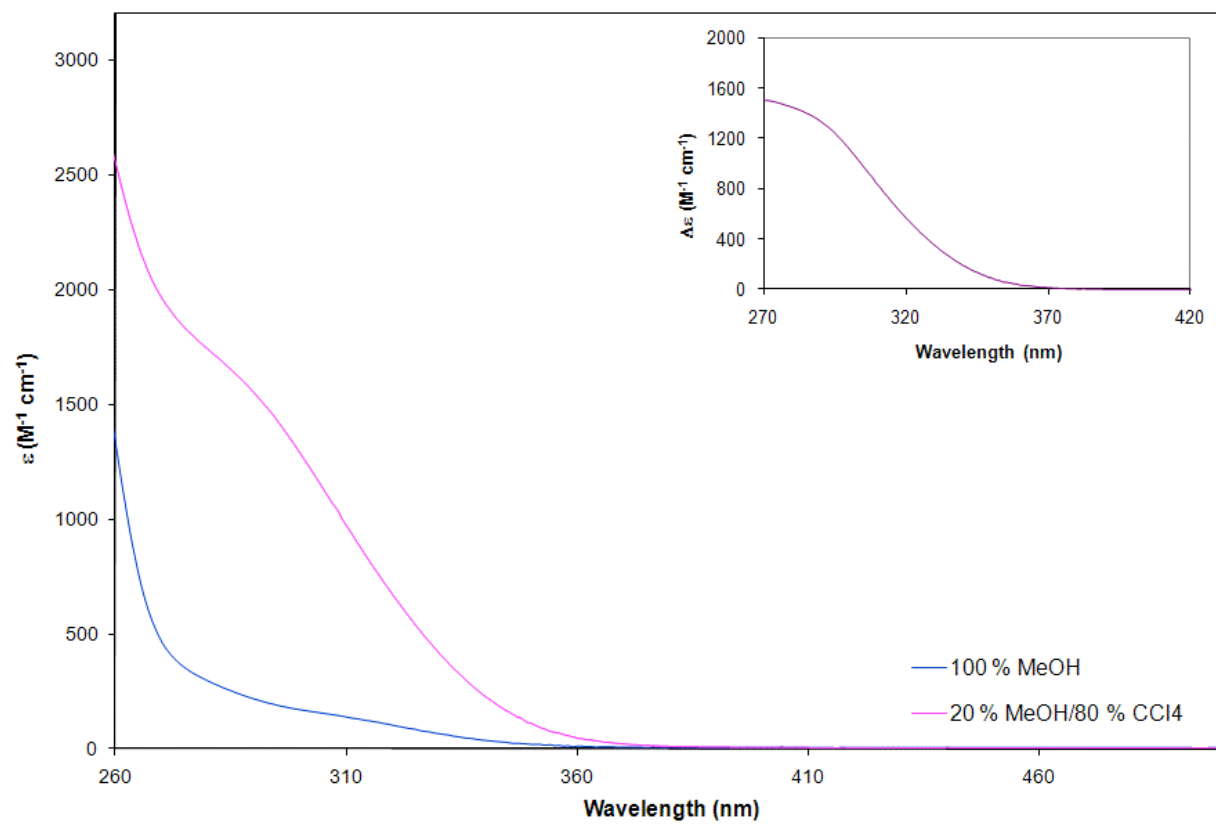


Table 4. ^1H Nuclear Magnetic Resonance Assignments of Benzoylosmocene.

Peak Position in ppm (splitting)	Identification
4.847 (s)	Cp
5.118 (t)	Cp'
5.301 (t)	Cp'
7.416 (t)	Phenyl
7.535 (t)	Phenyl
7.831 (d)	Phenyl

Figure 10.

Photoinitiated Anionic Polymerization of a Solution of Osmocene Dissolved in Ethyl 2-Cyanoacrylate.



Table 5. Relative Rates (t_{poly}) of Anionic Photoinitiation of Osmocene and Benzoylosmocene

Irradiated with White Light (>290 nm).

Sample	mM	t_{poly} (sec)
Oc	5.00	250
	2.49	>3720 ^a
BOc	4.88	330

^aWith 494 ppm methanesulfonic acid

Table 6. Relative Rates (t_{poly}) of Anionic Photoinitiation of Group 8 Metallocenes.

Sample	mM	t_{poly} (sec)
Fc ^a	10.3	4347
Rc ^a	9.9	234
Oc ^a	10.2	2840
BOc ^a	5.65	> 6900
BFc ^{16,b}	1.90	> 900
DFc ^{16,b}	1.61	38

^aPerformed at 365 nm. Light intensity = 4.5×10^{-8} ein/sec

^bPerformed at 436 nm. Light intensity = 7.8×10^{-8} ein/sec

CHAPTER 4
DISCUSSION ON THE PHOTOCHEMISTRY OF GROUP 8 PARENT METALLOCENES
AND THEIR BENZOYL DERIVATIVES

Photochemical Mechanism of the Group 8 Parent Metallocenes and their Derivatives

The nature of the bonding in the excited state of the benzoyl-substituted group 8 metallocenes can explain the various differences in their photochemistry (Scheme 2). BFc and DFc are very photoreactive compared to the other group 8 metallocenes and derivatives that have been studied. The charge-separated excited state reduces the hapticity of the metal-ring bond and allows for cleavage upon irradiation in non-halogenated solvents (Scheme 2). Nucleophilic solvents attack the metal center, giving a solvated iron(II) half-sandwich compound. Breaking of the metal-ring bond leads to the production of a benzoylcyclopentadienide anion which can be used to initiate anionic polymerization. From previous studies, it was seen that only the benzoylferrocenes undergo metal-ring bond cleavage.

While the excited state of the benzoyl-substituted ruthenocene and osmocene compounds does result in a reduction of the hapticity of the Cp ring, these compounds do not undergo metal-ring bond cleavage. The greater covalency of the Ru and Os metal centers increases the bond strength between the metal and the Cp rings in the ground state. This bonding could be residual in the excited state and as such make it harder to break the bond between the metal and the ring.

Furthermore, in the excited state it is possible that the benzoyl substituent is anchored to the metal center through an exocyclic bond (Figure 11). This exocyclic bond is more significant in R_c and O_c because the 4d and 5d orbitals have greater radial extension which allows for better

overlap with the π orbitals of the carbon-carbon double bond. Thus, metal-ring bond cleavage is very inefficient. These compounds are similar to the parent metallocenes and undergo photooxidation via a CTTS mechanism as seen in Scheme 2.

In good electron-accepting solvents, such as CCl_4 , the parent metallocenes showed evidence of CTTS transitions centered at 355 nm, 319 nm, and 275 nm (Fc, Rc, and Oc respectively.) Though steps were taken to find CTTS transitions in the benzoylmetallocenes in CCl_4 , no new peaks appeared. Instead, the CTTS transitions occur at shorter wavelengths and are obscured by more intense CT bands.

Since the efficiency of electron transfer follows the ease of oxidation of the metal centers, Rc and Oc are more efficient photooxidizers than their benzoyl-substituted derivatives due to the electron-withdrawing nature of the benzoyl group (Table 5).

Of the group 8 benzoylmetallocenes, the best anionic photoinitiator is DFc. Breaking the metal-ring bond gives the highly reactive benzoylcyclopentadienide anion which was seen to induce polymerization of CA very efficiently (Table 6). Comparing the ability of the benzoylferrocenes to that of the parent metallocenes or benzoylosmocene (Table 6), it can be seen that the metal-ring bond cleavage pathway is much more efficient than the CTTS photooxidation in photoinitiating anionic polymerization of CA.

BRc, DRc, and BOc, while having appreciable CT character, are poor photoinitiators for anionic polymerization due to the use of a less efficient CTTS pathway. Ground state and excited state properties work to increase the bonding between the metal and the ring, reducing the chance for metal-ring bond cleavage to occur. Hence, the only photochemical pathway available is that of a less effective CTTS photooxidation (Scheme 2). The reason that this pathway is less efficient is because the benzoyl groups make the molecule more stable toward oxidation.

It is interesting that R_c is the most efficient at using the CTTS pathway as R_c has the highest 1-electron oxidation potential of the parent metallocenes (+0.47 V, +0.83 V, and +1.03 V for F_c, O_c, and R_c respectively).³⁶ The greater efficiency of R_c compared to the other group 8 parent metallocenes is not clear, however, the following is a discussion of some possible explanations.

First, the oxidation of F_c is known to be reversible. Thus, in the [F_c:CA] complex the F_c delivers an electron to CA, yet the oxidized form may quickly undergo back electron transfer from the CA radical anion. In this way, very little CA is able to initiate polymerization because the product of the CTTS transition is quickly transforming back to the neutral species.

Secondly, R_c is well-known to undergo a 2-electron, irreversible oxidation.³⁷ (In fact, it took quite an effort to determine the 1-electron oxidation of R_c as by most other processes it underwent 2-electron oxidation every time.³⁶) Therefore, R_c is likely to undergo a secondary process where a second oxidation of R_c occurs.

Concluding Remarks

In this study, we found that adding an electron-withdrawing group onto one of the Cp rings of O_c introduces MLCT character. The mixing of more ligand character into the predominantly metal-based orbitals relaxes the Laporte selection rules and thus the low-energy bands are of higher intensity. Resonance Raman spectroscopy supports the view that there is charge-separation in the excited state. This charge-separation explains why the bands shift in solvents of varying polarity. Another consequence of the MLCT character is that the hapticity of the metal-ring coordination is reduced, thus weakening the metal-ring bonding and leaving the metal susceptible to attack by a nucleophilic solvent (Figure 3). Interestingly enough, however, BO_c does not favor a metal-ring bond cleavage pathway. It was also seen that O_c forms a

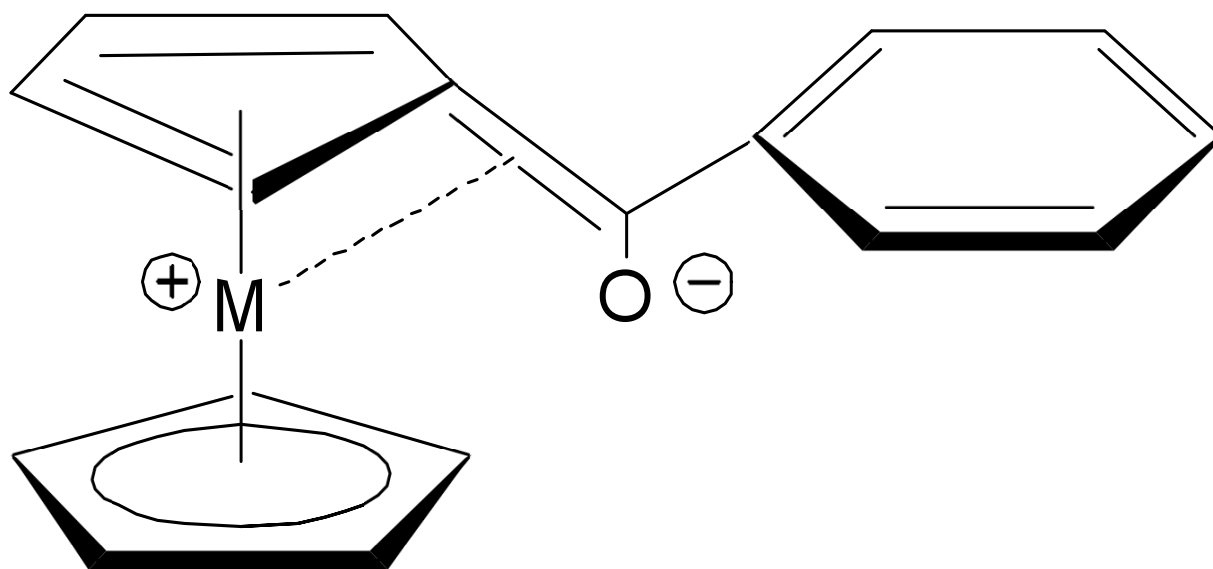
ground-state donor-acceptor complex in mixed solutions of CCl_4 , a good electron-accepting solvent, and MeOH. Since CA is also a good electron-accepting solvent, excitation into the absorption band of the donor-acceptor complex leads to CTTS photooxidation and subsequent polymerization of CA by the radical anion. This same pathway was more efficient than metal-ring bond cleavage for the BOc compound (Scheme 2).

The preference for a CTTS pathway over metal-ring bond cleavage is an effect of the osmium metal center. The strength of the metal-ring bond in the electronic ground state increases in the heavier metals of the group (i.e., Ru, Os). Greater residual bond strength is present in the excited state, therefore the bond between the metal and the ring is stronger for BRc, DRc, and BOc compared to BFc and DFc.^{6,17} Also, in the excited state, it is possible for the metal and double bond between the ring and carbonyl to be coordinated (Figure 11). The greater radial extension of the 5d orbitals of BOc allows for overlap with the exocyclic double bond and therefore keeps the ring tightly anchored to the metal in the charge-separated excited state. Though the benzoyl group gives the compound MLCT character, which would imply weakening of the bond due to charge-separation, it is harder to remove the substituted Cp ring due to the presence of an exocyclic bond in the excited state. Hence, BOc prefers a CTTS pathway instead of the more effective metal-ring bond cleavage pathway.

Furthermore, Oc is a more efficient photoinitiator compared to BOc owing to the ease of oxidizing the molecule. In good electron-accepting solvents like CCl_4 or CA, a ground-state donor-acceptor complex is formed between the solvent and the metallocene. When the donor-acceptor complex is irradiated with white light, the metallocene is oxidized and CA reduced which then initiates polymerization. Even with 365 nm light, where BOc is known to absorb, Oc

outperforms it in polymerizing CA (Table 6). The electron-withdrawing benzoyl group makes BOc harder to oxidize; therefore Oc is a better photoinitiator than BOc.

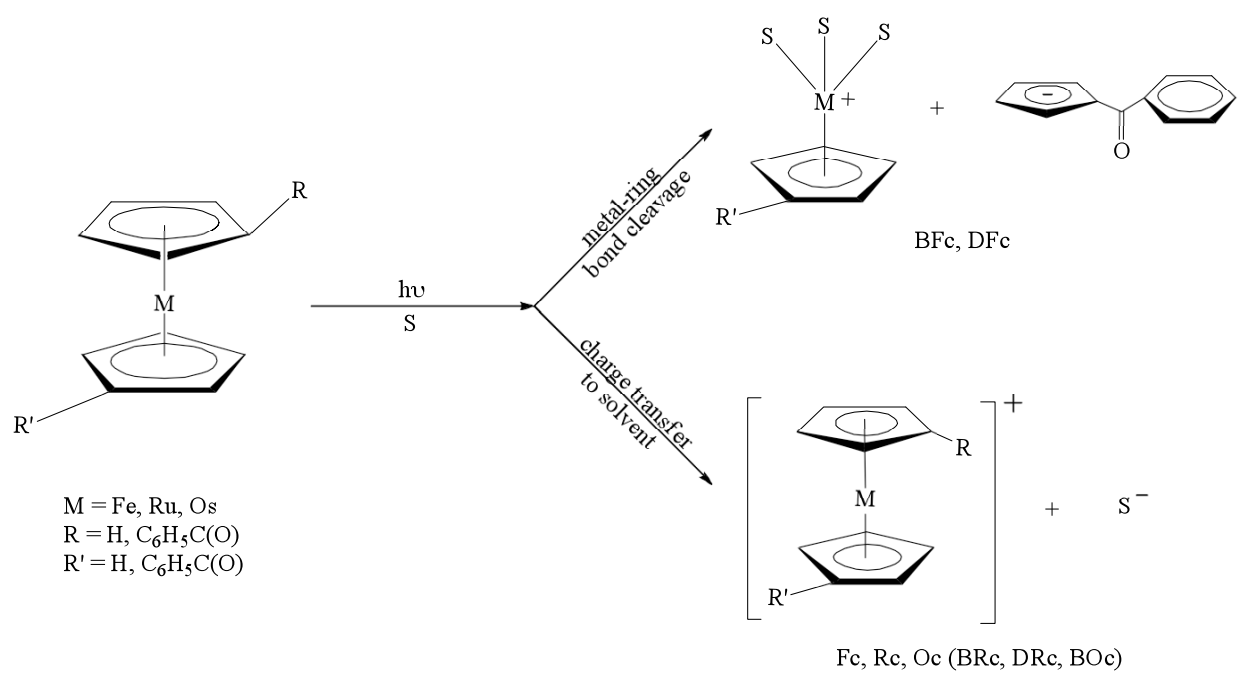
Figure 11.
Possible η^6 -fulvene Resonance Structure in the Excited State of Benzoylruthenocenes and
Benzoylosmocene.³⁹



$M = \text{Ru}, \text{Os}$

Scheme 2.

Photochemical Mechanism of the Group 8 Parent Metallocenes and Their Benzoyl Derivatives.



CHAPTER 5
PHOTOOXIDATION OF METHYLATED FERROCENE AND RUTHENOCENE
DERIVATIVES

Since the parent metallocenes and the benzoylruthenocenes and BOc had a propensity for CTTS photooxidation, we decided to take a deeper look at this photochemical mechanism. As such, we employed the electron-donating methyl groups to make the molecule easier to oxidize and to enhance the formation of a ground-state donor-acceptor complex. The following are the results of that study.

Electronic Absorption Spectra

The spectrum of decamethylferrocene (DMFc) is compared to ferrocene in ACN (Figure 12). The 445 nm band in Fc, corresponding to ${}^1A_{1g} \rightarrow {}^1E_{1g} + a^1E_{2g}$ ligand field transitions is shifted to 422 nm in DMFc in ACN. The second transition, ${}^1A_{1g} \rightarrow b^1E_{2g}$, is a shoulder on the high intensity LMCT band which has shifted to lower energy owing to the electron-donating nature of the substituents.⁴⁰

Since we undertook this study to increase the reactivity toward photooxidation, we considered the spectra of DMFc dissolved in various amounts of CCl₄ and ACN (Figure 13). As can be seen, a new absorption feature appears around 335 nm. This new feature is attributed to the formation of a ground-state donor-acceptor complex between DMFc and CCl₄.

Similarly, Rc undergoes only minor spectral changes with the presence of electron-donating methyl groups in ACN (Figure 14). The low-energy transition, ${}^1A_1' \rightarrow a^1E_1'' + E_2''$, has shifted to higher energy owing to the greater electron density on the rings.⁴⁰ Furthermore, the

LMCT band has shifted to lower energy and obscured the second ligand field transitions of ${}^1A_1' \rightarrow b^1E_1''$.

The spectra of DMRC in various solutions of CCl_4 and ACN are shown in Figure 15. A new absorption feature attributed to a CTTS transition is shown in the difference spectra (Figure 15, inset). From this data, we concluded that DMRC was capable of forming a ground-state donor-acceptor complex with the good electron-acceptor, carbon tetrachloride.

Formation Constants of Donor-Acceptor Complexes

Utilizing the Benesi-Hildebrand method,⁴¹ formation constants for ground-state donor-acceptor complexes can be calculated. First, we compared our results of the formation constant of a $[Rc:CCl_4]$ donor-acceptor complex in MeOH with the value previously reported.⁴² Next, we extended this same solvent system to Oc. We intended to extend the same treatment to the decamethylmetallocenes, however, these compounds proved to be thermally unstable in MeOH. Instead, to better compare formation constants, a full treatment of the group 8 parent and decamethyl-substituted metallocenes was undertaken in CCl_4 with ACN as the inactive solvent.

The equilibrium constant for the formation of a $[Rc:CCl_4]$ complex using methanol as the inactive solvent was calculated to be 1.64 ± 0.58 mol fraction⁻¹ which is within experimental error of the previously recorded value of 1.80 ± 0.15 mol frac⁻¹.⁴² For each mixture of Oc in CCl_4 and methanol, the K values were calculated using a range of wavelengths from 270 - 315 nm. The average equilibrium association constant for the formation of the $[Oc:CCl_4]$ complex is 1.33 ± 0.41 mol fraction⁻¹. While a direct comparison of Traverso and Scandola's¹⁰ value for an $[Fc:CCl_4]$ complex, 1.5 ± 0.2 mol fraction⁻¹, cannot be made due to the use of a different inactive solvent, the equilibrium constant is similar to those for the other two group 8 metallocenes. From

these values, it can be seen that the ground-state donor-acceptor complexes have similar stabilities.

We decided to investigate the possibility of a ground state donor-acceptor complex between the decamethyl derivatives and CCl_4 . DMFc was not thermally stable in MeOH solution, but was stable in ACN. Therefore, formation constants were calculated using solutions of ACN and CCl_4 (Table 7).

Though the values for the formation constants have large error limits, the calculations were performed correctly. For one, preliminary calculations for R_c in CCl_4 with MeOH as an inactive solvent instead of ACN agreed well with the published values.⁴² Secondly, the component calculations seemed reasonable. These calculations include calculating a $y = mx + b$ graph for every fifth wavelength of the CTTS transition. For example, the difference spectra was consulted and if the CTTS transition occurred over 270 nm – 300 nm then the Benesi-Hildebrand calculation would begin at 270 nm. The next wavelength under scrutiny would be 275 nm, then 280 nm, and so on. A $y = mx + b$ line would be calculated for every wavelength considered and from the equation the formation constant was calculated. The correlation constants were very reasonable, $r^2 > 0.85$, for every wavelength considered in each of the compounds. For this reason, we are confident in the individual values of the formation constants for each wavelength considered of each compound. However, never did the value of the formation constants plateau across the range of wavelengths. Instead, they increased fairly linearly. As such, the calculated average formation constants have large deviations.

While no decisive comparison can be made, it can be said that the parent metallocenes have similar stabilities as was seen when MeOH was the inactive solvent. Also, from the values of the formation constants, the complex formed by DMFc is more stable than that formed by Fc.

This behavior was evidenced by the fact that DMFc was able to initiate the polymerization of CA thermally. DMFc was also capable of thermally setting CA, though it took much longer to do so.

Therefore, it was seen that the addition of methyl groups to the Cp rings increased the formation of a ground-state donor-acceptor complex between DMFc and CCl_4 compared to Fc in the same solvents. The parent metallocenes appeared to have similar formation constants in two different inactive solvents. While this study was undertaken to enhance the CTTS photooxidation, the addition of methyl groups increased the reactivity of the compounds so much that they reacted thermally with CA.

Figure 12.

Electronic Absorption Spectra of Decamethylferrocene and Ferrocene in Acetonitrile.

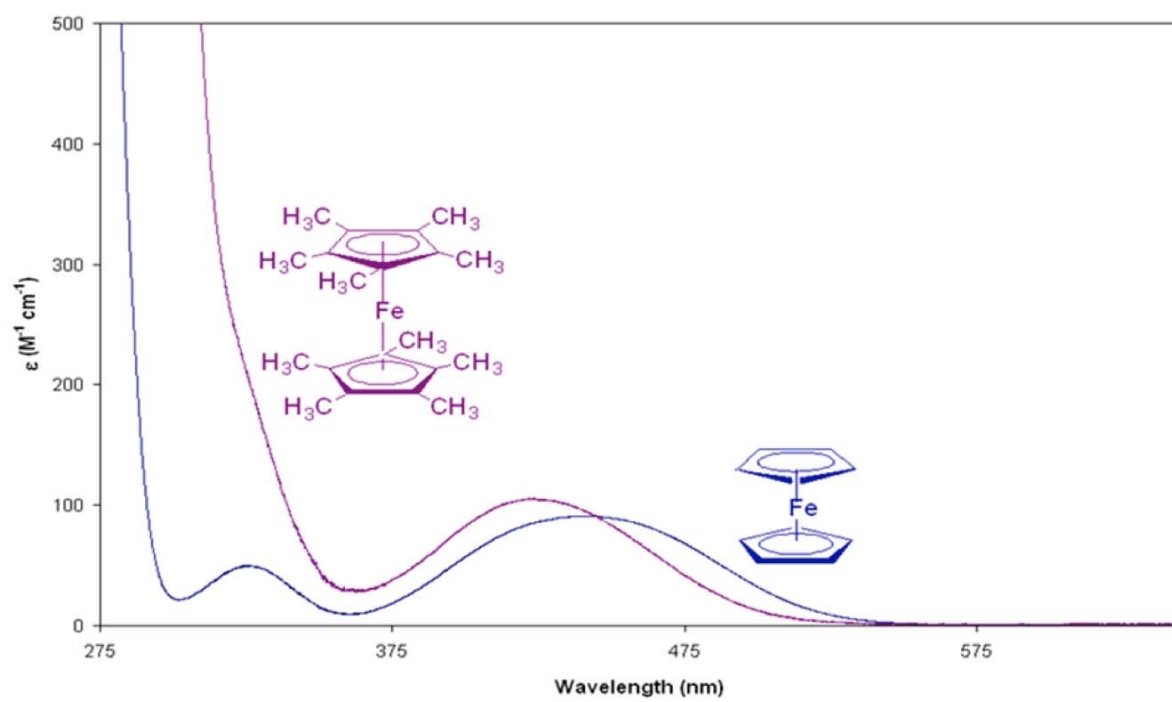


Figure 13.

Electronic Absorption Spectra of Decamethylferrocene Dissolved in Acetonitrile:Carbon Tetrachloride Mixtures. The inset is the difference spectrum showing a new absorption feature indicative of a CTTS transition.

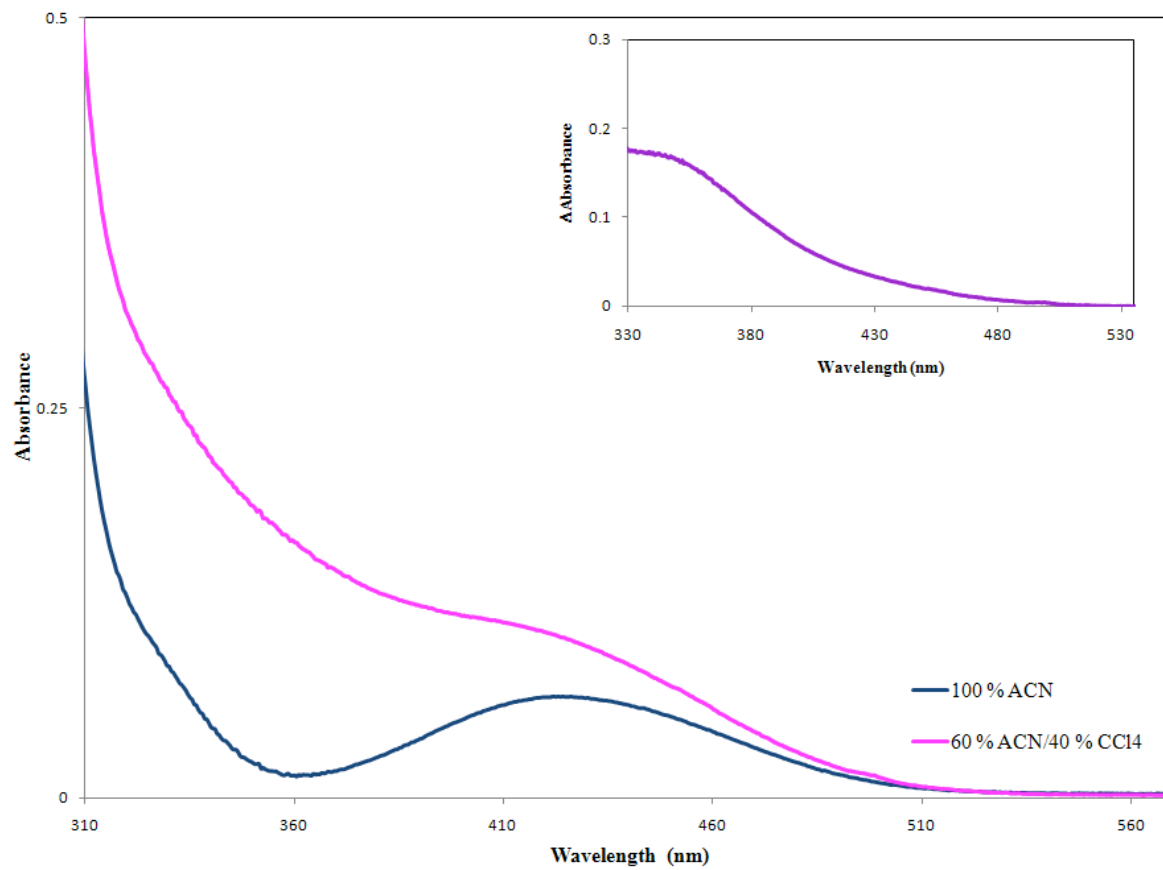


Figure 14.

Electronic Absorption Spectra of Decamethylruthenocene and Ruthenocene in Acetonitrile.

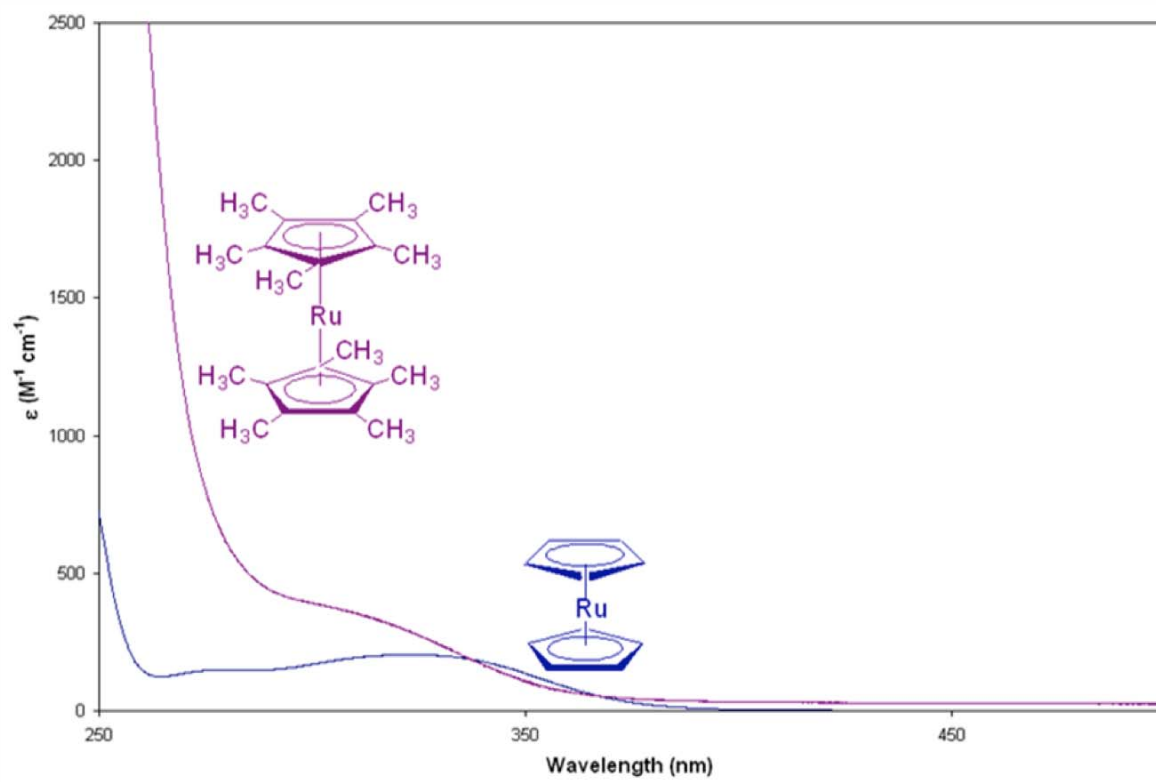


Figure 15.

Electronic Absorption Spectra of Decamethylruthenocene Dissolved in Acetonitrile:Carbon Tetrachloride Mixtures. The inset is the difference spectrum showing a new absorption feature indicative of a CTTS transition.

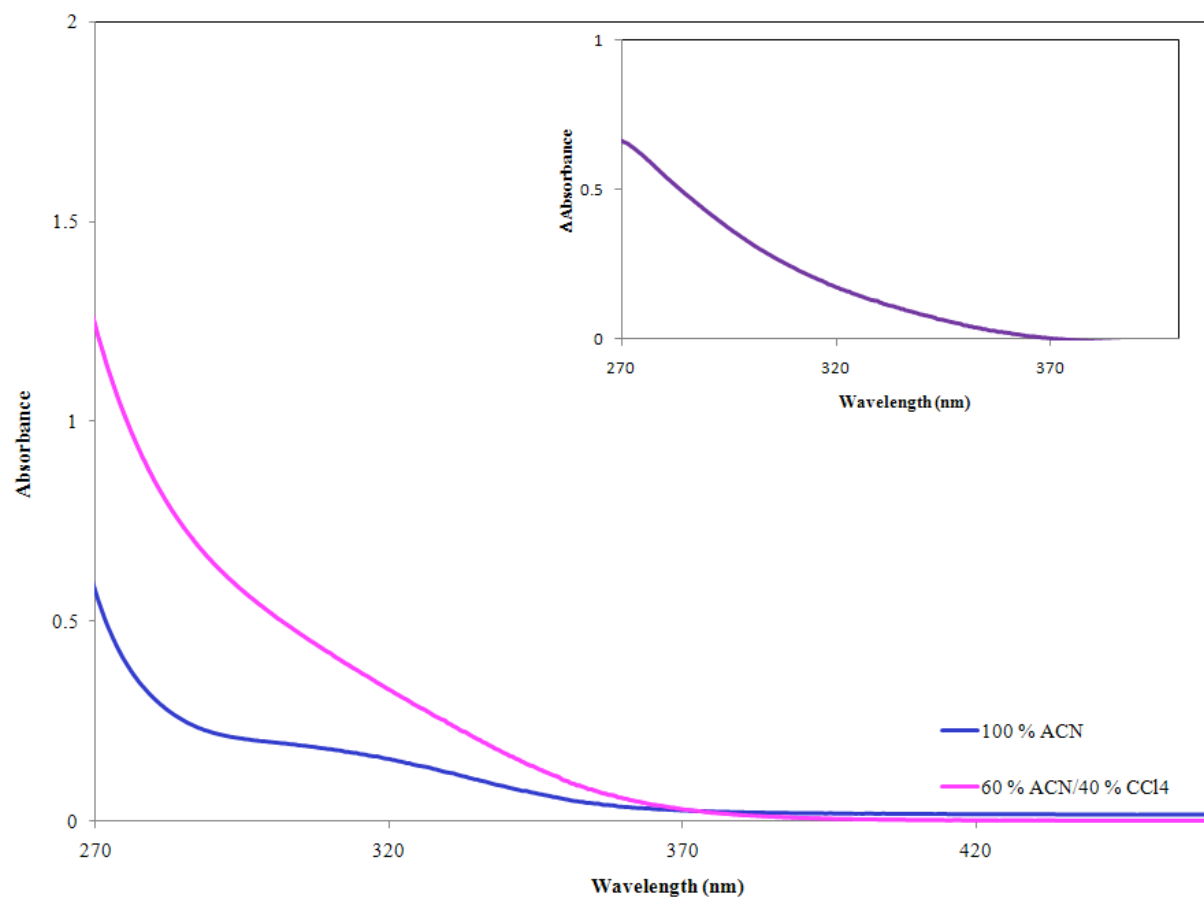


Table 7. Formation Constants of a Donor-Acceptor Complex Formed Between a Group 8 Metallocene and Carbon Tetrachloride in Acetonitrile:Carbon Tetrachloride Mixtures.

Sample	K (mol. frac.⁻¹)
Fc	0.53 ± 0.23
Rc	0.92 ± 0.33
Oc	0.60 ± 0.33
DMFc	1.66 ± 0.58
DMRc	1.11 ± 0.30

CHAPTER 6

ETHANE-BRIDGED [2]FERROCENOPHANE

Attempted Synthesis of Ethane-Bridged [2] Ferrocenophane

Synthesizing $\text{Fc}(\text{CH}_2)_2$ proved to be quite difficult. Nearly a year was spent trying to perfect the steps, many aspects of the reaction evolved (temperatures, addition of HMPA, making of NaCp), but nothing changed the fact that no product ever condensed onto the cold finger during sublimation. For the first few months, just making the lithiated ligand was a challenge.

These difficulties were not unforeseen. The 1,2-dicyclopentadienylethane ligand is very temperature sensitive and will easily rearrange to a more stable, spirocyclic compound. The original synthesis⁴³ called for the distillation of solvents to get the oil. Considering the thermal instability, it was no wonder that when this method was used no oil was found once all of the solvents (including THF, bp: 66 °C) had been distilled off.

After a considerable amount of time was spent working to keep the solution cold during separation and drying steps and still not getting any ligand, the Manners group, who had successfully synthesized the compound,³¹ was consulted. A new step was added where HMPA was used to entrap Na^+ , thus making the Cp anions of NaCp more reactive to 1,2-dibromoethane.³¹ This addition gave a dark red-yellow oil and, after lithiation, a white solid, both of which were a marked improvement.

However, when this white solid was put in THF it did not dissolve. When it was added to the iron(II) chloride slurry, it appeared to give a red product. This product decomposed upon vacuum sublimation around 60-70 °C. Nothing collected on the cold finger.

Once again, the Manners group was consulted and it was suggested that the initial reactant, NaCp, would have to be made. Originally, NaCp had been ordered as a 2.0 M solution in THF. However, Manners group noted their own problems when using the chemical and had resorted to making their own based on Roesky's method.³⁰ This change was made, however there was no appreciable product formation. At this point, after a year had passed, I stepped back and began to question if this type of synthesis was possibly out of the scope of my ability.

The next step was to scrutinize the individual steps, the first of which was the synthesis of NaCp. A new batch of NaCp was made by following Roesky's method. The ¹H NMR showed many peaks, but none were found at the frequency previously reported for NaCp, δ 5.60 ppm.³⁰ There were no peaks corresponding to any kind of carbon ring species (δ 5-7 ppm). The same results were seen for samples of what was thought to be the lithiated ligand and the final ferrocenophane product.

We are not a synthetic group, so it is likely that much of the problem lay in my own inexperience in dealing with air- and moisture-sensitive compounds. Seeing as how no product had been made over the course of a year, it was decided that studying the photochemistry of this compound was not feasible at this time. As such, we turned to the methylated derivatives to further explore the photochemistry of the group 8 metallocenes.

CHAPTER 7

CONCLUDING REMARKS

The studies performed on the group 8 metallocenes and their substituted derivatives lead us to some interesting conclusions. The presence of the electron-withdrawing benzoyl group introduces MLCT into the low-energy excited states of the parent metallocenes. This MLCT character gives a charge-separated excited state (Figure 3) that leads to heterolytic metal-ring bond cleavage in the benzoylferrocenes. This bond cleavage is not efficient in the benzoylruthenocenes or benzoylosmocene due to stronger residual bonding and the significance of a η^6 -fulvene exocyclic bond in the excited state (Figure 11).

The group 8 parent metallocenes form ground state donor-acceptor complexes with good electron-accepting solvents, such as CCl_4 or CA, leading to photooxidation via a CTTS excited state. This pathway also appears to be responsible for the photoinitiation of CA by the benzoylruthenocenes and benzoylosmocene, but this process is not efficient owing to the benzoyl groups making the metal center more stable towards oxidation.³⁷

The methylated metallocenes form ground-state donor-acceptor complexes with CCl_4 and presumably with CA. However, they are not thermally stable in CA and initiate polymerization in the dark. Therefore, they are not practical photoinitiators.

Many attempts were made to synthesize the bridged ferrocenophane, $\text{Fc}(\text{CH}_2)_2$, by published procedures.^{31, 43} However, the compound proved harder than originally thought to synthesize. As such, the photochemical behavior of $\text{Fc}(\text{CH}_2)_2$ has yet to be determined.

This study was begun with the intention to increase the mechanistic understanding of the group 8 metallocenes as well as expand the number of anionic photoinitiators available. BOc was synthesized and the low-energy excited states were characterized as having MLCT character using electronic absorbance spectroscopy. Solvent studies showed that the absorbance bands were solvent sensitive, indicative of a charge-separated excited state (Figure 3). The resonance Raman spectral studies also showed BOc has a charge-separated excited state. Quantum yield limits were determined for the photoreaction of Oc and BOc using ^1H NMR. This technique showed that Oc and BOc were photoinert in non-halogenated solvents. The possibility of CTTS transitions in solutions of CCl_4 was studied. Oc formed a ground-state donor-acceptor complex with the solvent, as shown by a new absorbance feature indicative of a CTTS transition. However a new absorbance was not so obvious in BOc solutions and must occur at higher energy.

The ability of BOc and Oc to initiate the polymerization of CA, as measured by t_{poly} , via a CTTS transition was considered. Also, t_{poly} values of some group 8 metallocenes at 365 nm were compared (Table 6). One particular wavelength was used to ensure that the intensity of the light was same for all the samples. From the data, it was seen that Rc was a better photoinitiator than the other group 8 metallocenes, though this result cannot be well explained.

Next, an ethane-bridged [2]ferrocenophane was studied. Unfortunately, a photochemical study of a bridged ferrocene cannot be considered with all of the other compounds. Though a lot of time and effort was spent on it, the synthesis of $\text{Fc}(\text{CH}_2)_2$ was not successful. Hopefully, this gap of knowledge of the group 8 metallocenes will be filled in the future.

Lastly, DMFc and DM Rc were examined with the idea that the electron-donating methyl groups would enhance the formation of a ground-state donor-acceptor complex with CCl_4 or CA.

Formation constants were calculated for the group 8 parent metallocenes as well as their decamethyl derivatives (Table 7). It can be seen that, within experimental error, the group 8 parent metallocenes have similar formation constants, and the formation constant for DMFc is higher than that of Fc.

Aside from formation constants, I studied the ability of the decamethyl-substituted group 8 metallocenes to initiate the polymerization of CA. DMFc and DMRc initiated polymerization of CA in the dark. This thermal instability reflects the higher formation constant of DMFc compared to Fc. Consequently, neither DMFc nor DMRc are useful photoinitiators.

REFERENCES

1. Kaur, M.; Srivastava, A. K., *J. Macromol. Sci.* **2002**, *C42* (4), 481-512.
2. Crivello, J. V., *Ann. Rev. Mater. Sci.* **1983**, *13*, 173-190.
3. Kutal, C., *Coord. Chem. Rev.* **2001**, *211*, 353-368.
4. Sanderson, C. T.; Palmer, B. J.; Morgan, A.; Murphy, M.; Dluhy, R. A.; Mize, T.; Amster, I. J.; Kutal, C., *Macromolecules* **2002**, *35* (26), 9648-9652.
5. Sohn, Y. S.; Hendrickson, D. N.; Gray, H. B., *J. Am. Chem. Soc.* **1971**, *93* (15), 3603-3612.
6. Yamaguchi, Y.; Ding, W.; Sanderson, C. T.; Borden, M. L.; Morgan, M. J.; Kutal, C., *Coord. Chem. Rev.* **2007**, *251*, 515-524.
7. Boulet, P.; Chermette, H.; Daul, C.; Gilardoni, F.; Rogemond, F.; Weber, J.; Zuber, G., *J. Phys. Chem. A* **2001**, *105*, 885-894.
8. Thander, A.; Mallik, B., *Proc. Indian Acad. Sci. (Chem. Sci.)* **2000**, *112* (4), 475-485.
9. Traverso, O.; Sostero, O.; Mazzocchin, G. A., *Inorg. Chim. Acta* **1974**, *11*, 237-241.
10. Traverso, O.; Scandola, F., *Inorg. Chim. Acta* **1970**, *4*, 493-498.
11. Sostero, S.; Duatti, A.; Zanella, P.; Traverso, O., *J. Organomet. Chem.* **1978**, *157*, 437-443.
12. Frey, J. E.; Du Pont, L. E.; Puckett, J. J., *J. Org. Chem.* **1994**, *59*, 5386-5392.
13. Vogler, A.; Kunkley, H., *Coord. Chem. Rev.* **1998**, *177*, 81-96.
14. Yamaguchi, Y.; Kutal, C., *Macromolecules* **2000**, *33* (4), 1152-1156.
15. Yamaguchi, Y.; Kutal, C., *Inorg. Chem.* **1999**, *38* (21), 4861-4867.

16. Yamaguchi, Y.; Palmer, B. J.; Kutal, C., *Macromolecules* **1998**, *31* (15), 5155-5157.
17. Sanderson, C. T.; Quinlan, J. A.; Conover, R. C.; Johnson, M. K.; Murphy, M.; Dluhy, R. A.; Kutal, C., *Inorg. Chem.* **2005**, *44*, 3283-3289.
18. Noviandri, I.; Brown, K. N.; Fleming, D. S.; Gulyas, P. T.; Lay, P. A.; Masters, A. F.; Phillips, L., *J. Phys. Chem. B* **1999**, *103* (32), 6713-6722.
19. Wang, W.-J.; Lay, Y.-L.; Chang, C.-S.; Chiu, H.-S., *Mol. Cryst. Liq. Cryst.* **2006**, *456*, 149-154.
20. Kudinov, A. R.; Rybinskaya, M. I.; Struchkov, Y. T.; Yanovskii, A. I.; Petrovskii, P. V., *J. Organomet. Chem.* **1987**, *336*, 187-197.
21. Morgan, M.; Kutal, C., *Unpublished results*.
22. Barlow, S.; Drewitt, M. J.; Dijkstra, T.; Green, J. C.; O'Hare, D.; Whittingham, C.; Wynn, H. H., *Organometallics* **1998**, *17*, 2113-2120.
23. Rulkens, R.; Gates, D. P.; Balaishis, D.; Pudelski, J. K.; McIntosh, D. F.; Lough, A. J.; Manners, I., *J. Am. Chem. Soc.* **1997**, *119*, 10976-10986.
24. Herbert, D. E.; Tanabe, M.; Bourke, S. C.; Lough, A. J.; Manners, I., *J. Am. Chem. Soc.* **2008**, *130*, 4166-4176.
25. Herbert, D. E.; Mayer, U. F. J.; Manners, I., *Angew. Chem. Int. Ed.* **2007**, *46*, 5060-5081.
26. Herberhold, M., *Angew. Chem. Int. Ed.* **1995**, *34*, 1837-1839.
27. Hatchard, C. G.; Parker, C. A., *Proc. R. Soc. London, Ser. A* **1956**, *235*, 518-536.
28. Rausch, M. D.; Fischer, E. O.; Grubert, H., *J. Am. Chem. Soc.* **1960**, *82*, 76-82.
29. Rausch, M. D.; Mark, V., *J. Org. Chem.* **1963**, *28*, 3225-3228.
30. Panda, T. K.; Gamer, M. T.; Roesky, P. W., *Organometallics* **2003**, *22*, 877-878.

31. Nelson, J. M.; Nguyen, P.; Peterson, R.; Rengel, H.; Macdonald, P. M.; Lough, A. J.; Manners, I.; Raju, N. P.; Greedan, J. E.; Barlow, S.; O'Hare, D., *Chem. Eur. J.* **1997**, *3* (573-584), 573.
32. Drozdowski, P. M.; Johnson, M. K., *Appl. Spectrosc.* **1988**, *42*, 1575-1577.
33. Kunkely, H.; Vogler, A., *Transition Met. Chem.* **2000**, *25*, 234-236.
34. Kimel'fel'd, Y. M.; Smirnova, E. M., *J. of Mol. Struct.* **1973**, *19*, 329-346.
35. Ding, W.; Sanderson, C. T.; Conover, R. C.; Johnson, M. K.; Amster, I. J.; Kutal, C., *Inorg. Chem.* **2003**, *42* (5), 1532-1537.
36. Hill, M. G.; Lamanna, W. M.; Mann, K. R., *Inorg. Chem.* **1991**, *30*, 4687-4690.
37. Kuwana, T.; Bublitz, D. E.; Hoh, G., *J. Am. Chem. Soc.* **1960**, *82*, 5811-5817.
38. Palleros, D. R., *Experimental Organic Chemistry*. John Wiley & Sons, Inc.: New York, NY, 2000.
39. Barlow, S.; Cowley, A.; Green, J. C.; Brunker, T. J.; Hascall, T., *Organometallics* **2001**, *20*, 5351-5359.
40. Ritsko, J. J.; Nielson, P.; Miller, J. S., *J. Chem. Phys.* **1977**, *67* (2), 687-690.
41. Benesi, H. A.; Hildebrand, J. H., *J. Am. Chem. Soc.* **1949**, *71*, 2703-2707.
42. Borrell, P.; Henderson, E., *J.C.S. Dalton* **1975**, 432-438.
43. Lentzner, H. L.; Watts, W. E., *Tetrahedron* **1971**, *27*, 4343-4351.